Synthesis and NaOTf Mediated Self-Assembly of Monodendritic Crown Ethers

Virgil Percec,*[a] Wook-Dong Cho,[a] Goran Ungar,[b] and Duncan J. P. Yeardley[b]

Abstract: The synthesis of ten benzyl ether based self-assembling monodendrons containing benzo[15]crown-5 at their focal point is presented. These dendritic building blocks self-assemble either directly or via complexation with NaOTf in two-dimensional smectic B, smectic A, and *p6mm* hexagonal columnar (Φ_h) and three-dimensional $Pm\bar{3}n$ cubic lattices. Retrostructural analysis of these lattices and of the lattices generated from the same monodendrons containing various other functional groups at their focal point by X-ray diffraction experiments provided for the first time a correlation between the molecular structure and the shape of the monodendron, the shape of the supramolecular dendrimer and the symmetry of the lattice. It has been shown that complexation with NaOTf provides the following five different trends: a) stabilization of the three-dimensional $Pm\bar{3}n$ cubic lattice self-organized from spherical dendrimers that are self-assembled from conic monodendrons; b) stabilization of the two-dimensional S_A phase generated from parallelepiped monodendrons; c) no effect on the stability of the two-dimensional S_B phase generated from parallelepiped monodendrons; d) stabilization of the two-dimensional *p6mm* hexagonal columnar phase self-organized from cylindrical supramolecular dendrimers that are self-assembled from tapered monodendrons; and e) destabilization of the two-dimensional *p6mm* hexagonal columnar phase self-organized from cylindrical supramolecular dendrimers self-assembled from half-disc monodendrons. Mechanisms of NaOTf mediated self-assembly processes were suggested. These monodendritic crown ethers and their NaOTf complexes provide the largest diversity of liquid crystalline phases encountered so far in any library of supramolecular dendrimers.

Keywords: crown compounds · dendrimers · lattices · self-assembly · supramolecular chemistry

Introduction

Dendrimers have emerged as one of the most influential architectural motif that provided substantial impact at the interface between various subdisciplines of chemistry such as biological mimics, catalysis, nanoelectronics, supramolecular chemistry, and chirality.[1]

We have elaborated a strategy for the synthesis of self-assembling monodendrons which can be equipped with various functionalities at their focal point.[2] These monodendrons self-assemble in supramolecular dendrimers that subsequently self-organize in lattices and superlattices. The retrostructural analysis of these lattices provides access to the determination of the shape and size of the supramolecular dendrimers and of their parent dendrons.[2e,f, n, 3j, k] These designed monodendrons are subsequently employed in the synthesis of more complex macromolecular systems. Depending on the position via which the monodendrons are attached to the polymer backbone (i.e., at the focal point or at their periphery) the complex macromolecular system results either in single molecule functional nanosystems[3] or a supramolecular barrier network containing multifunctional channels that mimic some of the functions of the cell membrane.[4]

The functionality most frequently employed at the focal point of these self-assembling monodendrons is a crown ether or a podant such as an oligooxyethylene group.[2a–e, g, o] Crown ethers have been incorporated at the focal point of monodendrons to facilitate self-assembly mediated by ionic interactions after complexation of the crown ether with suitable metal salts.[2a–e] The resulting supramolecular columnar systems are equipped with an ion channel penetrating through their core that facilitates selective ion transport.[2a, c] These crown ether containing monodendrons are also precursors to supramolecular networks functionalized with ion-selective channels.[4] None of the previously reported dendritic crown ethers self-assemble in the absence of complexation.[2a–d]

[a] Prof. V. Percec, Dr. W.-D. Cho
Roy & Diana Vagelos Laboratories, Department of Chemistry
University of Pennsylvania, Philadelphia, PA 19104-6323 (USA)
Fax: (+1) 215-573-7888
E-mail: percec@sas.upenn.edu

[b] Dr. G. Ungar, Dr. D. J. P. Yeardley
Department of Engineering Materials and
Center for Molecular Materials, University of Sheffield
Sheffield, S1 3JD (UK)

  0947-6539/02/0809-2011 $ 20.00+.50/0

Exception from this group of molecules is provided so far only by a class of semifluorinated crown ether containing dendrons that are able to self-assemble in the absence of the complexation process via the fluorophobic effect.[2e, g] In principle, the fluorophobic effect can be replaced by suitable nonfluorinated monodendrons of higher generation.

This publication reports the synthesis and retrostructural analysis of the first library of crown ether containing monodendrons that self-assemble and subsequently self-organize into two-dimensional *p6mm* hexagonal columnar, smectic B and smectic A, as well as in three-dimensional $Pm\bar{3}n$ cubic lattices either in the absence of complexation with NaOTf or mediated by the complexation with NaOTf. The results described here will elucidate the correlation between the molecular structure of the nonfunctionalized and crown ether functionalized monodendrons, their capability to self-assemble and the shape of these molecular building blocks and of their supramolecular assembly. These experiments also provide the largest diversity of liquid crystalline phases based on dendritic building blocks since our pioneering report on liquid crystalline dendrimers and their model hyperbranched polymers.[5] In addition, these results may open new avenues towards the elaboration of novel catalytic and ion-conductive, ion-active and ion-selective principles based on self-assembling monodendritic crown ethers.

Results and Discussion

Synthesis of dendritic crown ethers: In a recent publication from our laboratory we have reported the synthesis, structural, and retrostructural analysis of three libraries of self-assembling benzyl ether monodendrons.[2n] Nine representative examples of monodendrons that were selected for the current synthetic experiments are shown in Scheme 1. Four of them **(3,4)12G1-CO_2H**, **(4-3,4)12G1-CO_2H**, **(3,4-3,4)12G2-CO_2H**, **(4-3,4,5-3,4)12G2-CO_2H** are based on 3,4-disubstitued benzyl ether AB_2 monodendrons containing various first-generation monodendrons (minidendrons) functionalized with *n*-dodecanyloxy groups on their periphery. Two of them, **(3,4-3,5)12G2-CO_2H** and **(4-3,4,5-3,5)12G2-CO_2H** are based on 3,5-disubstituted benzyl ether AB_2 monodendrons with various minidendrons on their periphery. The last three, **(3,4-3,4,5)12G2-CO_2H**, **(3,4,5-3,4,5)12G2-CO_2H**, and **(4-3,4,5-3,4,5)12G2-CO_2H** are based on 3,4,5-trisubstituted benzyl ether AB_3 monodendrons. All carboxylic acid monodendrons were obtained by the saponification of their corresponding methyl ester. The synthesis of methyl ester precursors and the corresponding carboxylic acids with the exception of **(4-3,4,5-3,4,5)12G2-CO_2H** were carried out as reported previously.[2f, h, n, 3b, 6–8] The synthesis of **(4-3,4,5-3,4,5)12G2-CO_2H** is described in the Experimental Section, while that of mono-

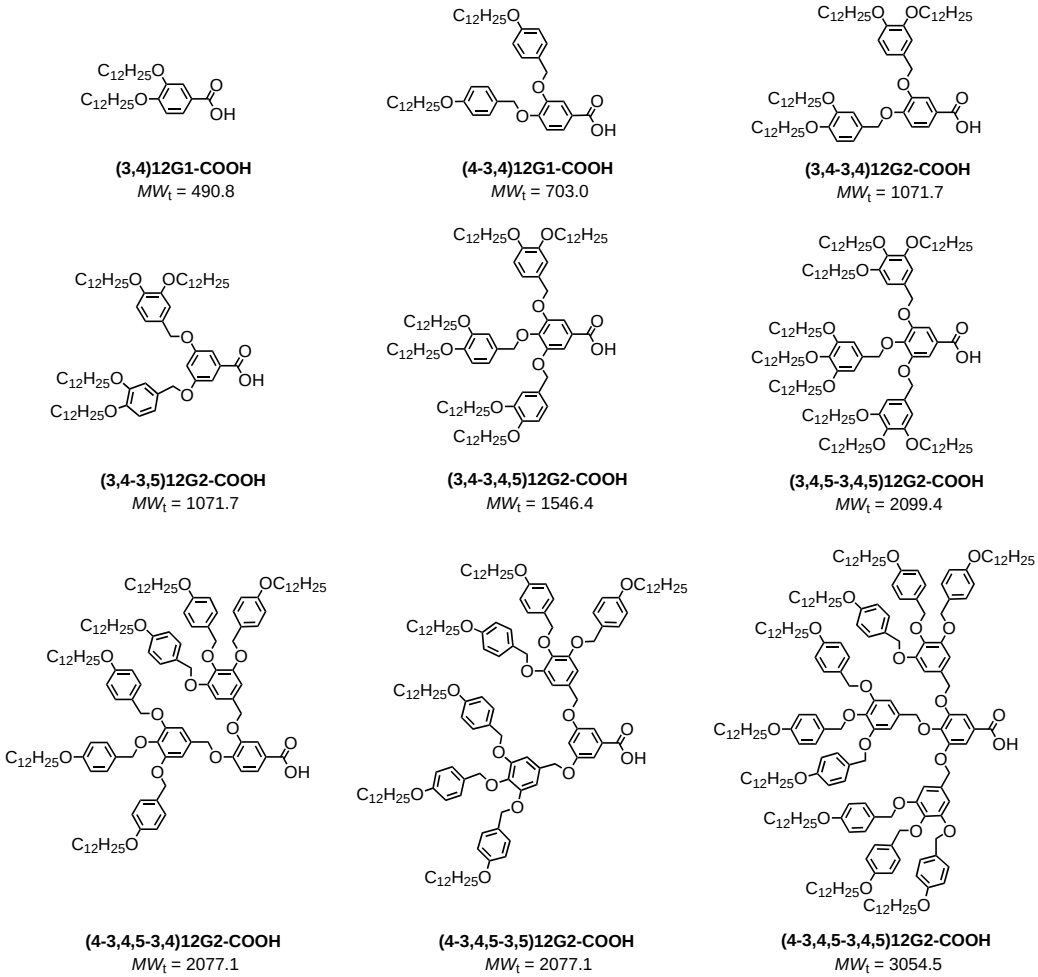

Scheme 1. Monodendrons containing carboxylic acid at the focal point.

0947-6539/02/0809-2012 $ 20.00+.50/0 *Chem. Eur. J.* **2002**, *8*, No. 9

dendritic crown ethers is outlined in Scheme 2. The monodendrons containing benzo[15]crown-5 at their focal point were synthesized by the estherification of the monodendritic carboxylic acids described in Scheme 1 with 4′-hydroxymethylbenzo[15]crown-5 in the presence of dicyclohexylcarbodiimide (DCC)/4-dimethylaminopyridinium *p*-toluenesulfonate (DPTS) in CH_2Cl_2. 4′-Hydroxymethylbenzo[15]crown-5 (**B15C5**) was synthesized as reported previously.[2a] All dendritic crown ethers were obtained as white solids in 48 to 83 % yield after purification by column chromatography (silica gel) and recrystallization.

The structural analysis of the supramolecular dendrimers and the retrostructural analysis of the corresponding monodendritic crown ethers was performed by a combination of techniques consisting of differential scanning calorimetry (DSC), thermal optical polarized microscopy (TOPM), and X-ray diffraction (XRD) experiments according to conventional methods employed in our laboratory.[2e, f, n, 5] DSC experiments are qualitatively identifying the monodendrons which self-assemble in supramolecular dendrimers and subsequently self-organize in two- and three-dimensional lattices. In addition they are providing the transition temperatures between various ordered states. The transition temperatures and the corresponding enthalpy changes of all compounds are summarized in Tables 1–3.

Subsequently, TOPM experiments are used to discriminate qualitatively between smectic or hexagonal columnar two-dimensional (fluid and optically anisotropic) and cubic three-dimensional (fluid and optically isotropic) or crystalline three-dimensional lattices (solid and optically anisotropic). Figure 1 shows selected examples of TOPM micrographs displayed by the smectic A and hexagonal columnar (Φ_h) two-dimensional

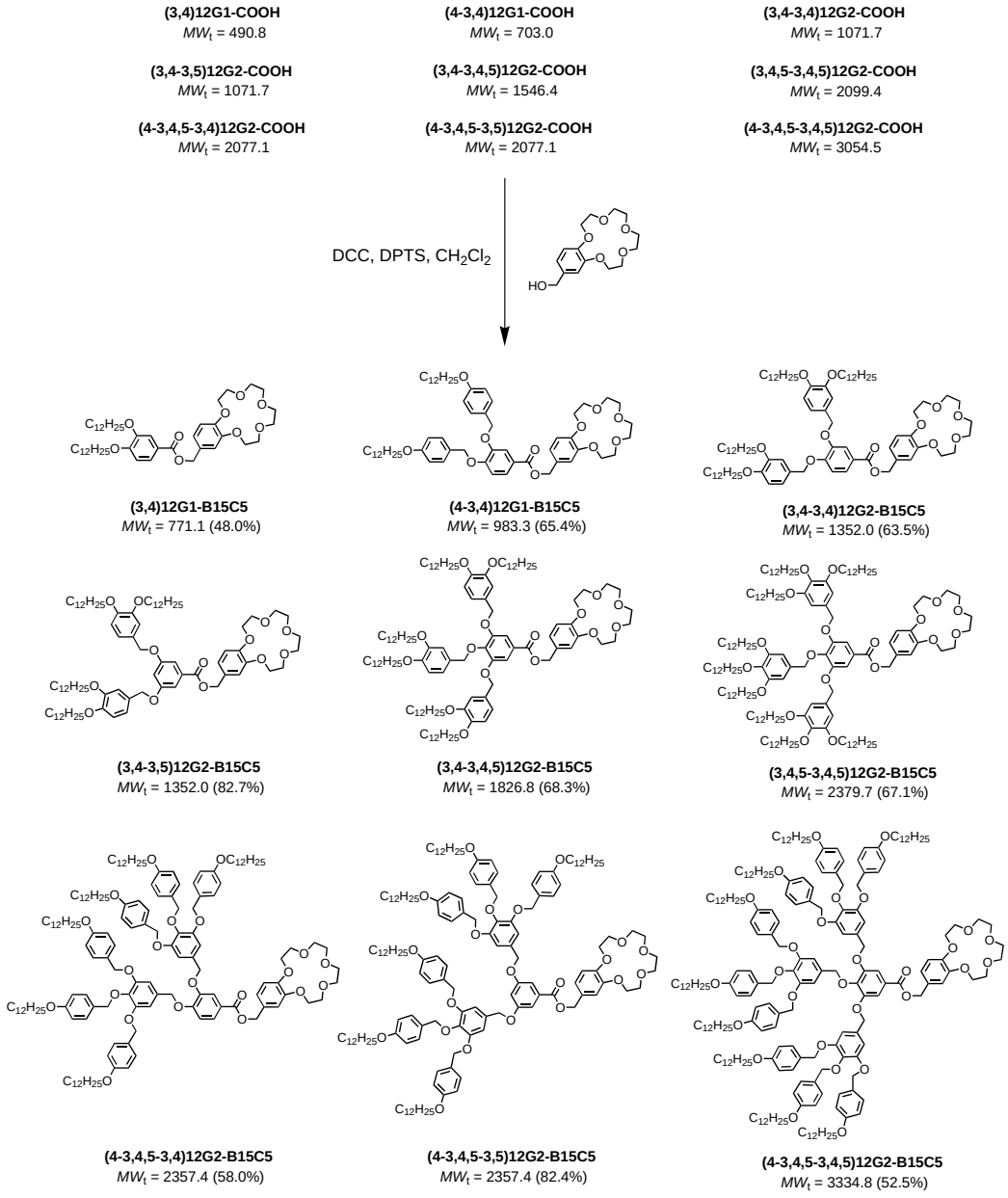

Scheme 2. Synthesis of monodendrons containing **B15C5** crown ether at their focal point.

Table 1. Thermal characterization of intermediary monodendrons.

Monodendron	Thermal transitions [°C] and corresponding enthalpy changes [kcal mol^{-1}][a]	
	Heating	Cooling
(3,4)12G1-CO_2CH_3	k[b] −2 (0.80) k 16 (2.93) k 54 (17.13) i[c] k 38 (1.16) −k 41 (3.69) k 54 (16.95) i	i 22 (13.58) k
(3,4)12G1-CO_2H	k 14 (14.64) k 94 (1.94) k 116 (13.12) i k 92 (0.94) k 116 (13.71) i	i 98 (14.32) k 87 (0.80) k
(4-3,4)12G1-CO_2CH_3	k 4 (1.96) k 60 (12.57) k 99 (4.87) i k 7 (1.64) k 55 (3.22) Φ_h[d] 60 (2.03) i	i 54 (1.92) Φ_h 2 (2.51) k
(4-3,4)12G1-CO_2H	k −9 (9.89) k 125 (18.17) i k −9 (1.19) k 125 (19.22) i	i 114 (1.00) Φ_h 110 (15.37) k
(4-3,4,5)12G1-CO_2CH_3	k 33 (7.83) k 60 (24.68) k 67 (7.90) i k 66 (29.00) i	i 40 (26.39) k
(4-3,4,5)12G1-CO_2H	k 47 (17.05) −k 58 (1.31) k 70 (11.82) Φ_h 145 (3.97) i k 43 (15.10) Φ_h 140 (3.71) i	i 136 (3.77) Φ_h 36 (15.43) k
(3,4-3,4)12G2-CO_2CH_3	k −6 (0.55) k 93 (22.27) i −k 27 (8.89) −k 52 (1.19) k 93 (23.16) i	i 78 (4.65) k −4 (0.93) k
(3,4-3,4)12G2-CO_2H	k 2 (0.31) k 88 (0.54) −k 97 (3.34) k 108 (17.58) Cub[e] 119 (0.47) i −k 86 (4.63) k 108 (22.68) Cub 118 (0.54) i	i 114 (0.40) Cub 67 (17.04) k
(3,4-3,5)12G2-CO_2CH_3	k 77 (32.29) i k 76 (28.39) i	i 41 (24.47) k
(3,4-3,5)12G2-CO_2H	k 69 (21.82) i k 14 (3.02) Φ_h 68 (3.94) i	i 63 (4.00) Φ_h 5 (2.45) k
(4-3,4,5-3,5)12G2-CO_2CH_3	k 54 (36.82) −k 66 (9.23) k 82 (0.22) i k −19 (7.95) Φ_h 71 (2.13) i	i 66 (2.15) Φ_h −23 (7.62) k
(4-3,4,5-3,5)12G2-CO_2H	k 35 (168.41) Cub[f] 196 (0.64) i k −19 (21.02) k 75 (3.34) Cub 195 (0.50) i	i 181 (0.17) Cub 64 (1.30) k −22 (8.28) k
(4-3,4,5-3,4,5)12G2-CO_2CH_3	k 47 (40.18) Φ_h 97 (2.28) LC[g] 118 (0.65) i k −16 (19.58) Φ_h 98 (2.19) LC 117 (0.52) i	i 107 (0.06) LC 91 (2.55) Φ_h −23 (13.61) k
(4-3,4,5-3,4,5)12G2-CO_2H	k −19 (16.03) k 182 (0.26) Cub[f] 195 (0.59) i[h]	
(3,4-3,4,5)12G2-CO_2CH_3	k −5 (27.04) k 61 (1.45) i k −3 (8.03) k 33 (0.41) i	i −8 (11.86) k
(3,4-3,4,5)12G2-CH_2OH	k 0 (2.42) k 60 (39.14) Cub[e] 133 (4.45) i k 42 (18.32) Cub 133 (4.30) i	i 128 (4.31) Cub 15 (20.49) k
(3,4-3,4,5)12G2-CO_2H	k −4 (8.22) k 61 (31.93) LC 138 (2.16) i k 11 (12.87) k 30 (2.25) k 49 (6.42) LC 129 (6.09) i	i 125 (2.01) LC 33 (5.68) k 2 (16.64) k
(3,4,5-3,4,5)12G2-CO_2CH_3	k 57 (37.00) i −k 10 (5.49) k 57 (36.70) i	i 35 (0.74) Cub[e] 11.4 (21.9) k
(3,4,5-3,4,5)12G2-COOH	k 85 (25.6) Cub[e] 119 (1.27) i k −9 (5.62) k 43 (−19.50) k 83 (24.30) Cub 117 (0.96) i	i 111 (0.87) Cub −15 (8.67) k
(4-3,4,5-3,4)12G2-CO_2CH_3	k −9 (2.41) k 51 (23.21) Cub[e] 119 (6.51) i k −27 (13.05) Cub 119 (4.96) i	i 114 (4.83) Cub −26 (13.11) k
(4-3,4,5-3,4)12G2-CO_2H	k 1 (5.85) k 39 (2.56) k 78 (8.55) Cub[e] 178 (4.74) i k −18 (3.73) g 31 k 62 (2.51) k 113 (0.08) Cub 178 (0.37) i	i 167 (0.11) Cub 51 (1.22) g[i] 22 k −22 (3.11) k

[a] Data from the first heating and cooling scans are on the first line and data from the second heating are on the second line. [b] k = crystalline. [c] i = isotropic. [d] $\Phi_h = p6mm$ hexagonal columnar lattice. [e] Cub = $Pm\bar{3}n$ cubic lattice. [f] Cub = $Im\bar{3}m$ cubic lattice. [g] LC = unknown lattice. [h] Decomposition after first heating. [i] g = glassy.

liquid crystalline lattices of selected examples of supramolecular dendrimers self-assembled and subsequently self-organized from dendritic crown ethers.

Structural and retrostructural analysis of supramolecular dendrimers: The quantitative structural and retrostructural analysis of supramolecular dendrimers and of their complexes with NaOTf performed by X-ray diffraction experiments according to the procedure outlined in Scheme 3 and described in detail previously.[2e, f, n, 3j, k, 5] The *d*-spacings of intermediary and crown ether containing monodendrons and their selected complexes with NaOTf are collected in Table 4. The lattice dimensions (a), the experimental densities (ρ_{20}), the experimental layer spacing of the smectic and the experimental diameter of columnar or spherical supramolecular dendrimers (D), the number of monodendrons per unit cell (μ') for the case of $Pm\bar{3}n$ and $Im\bar{3}m$ lattices, the number of monodendrons per spherical dendrimer (μ) for the case of $Pm\bar{3}n$ and $Im\bar{3}m$ lattices or per 4.7 Å[9] column stratum of the $p6mm$ lattice and the planar angle (α') that represents the projection of the solid angle, α (where $\alpha = 4\pi/\mu$), of the conical and tapered monodendrons (where $\alpha' = \alpha/2 = 2\pi/\mu$)[2j, m, n] are reported in Table 5. The results from Table 5 were used to generate the mechanisms of self-assembly illustrated in Scheme 4.

We will discuss in more detail the most representative examples of monodendritic crown ethers by following their DSC traces on which all phases marked were assigned by XRD analysis. Figure 2 shows representative DSC traces of **(3,4)12G1-B15C5** and of its complexes with NaOTf. **(3,4)12G1-B15C5** is crystalline. Its complexation with 0.2 mol NaOTf changes completely its phase behavior. On cooling from the isotropic state **(3,4)12G1-B15C5·NaOTf** = 0.2 exhibits a Φ_h followed by a S_B phase. On reheating the S_B phase undergoes isotropization followed by an immediate crystallization process. The resulting crystal phase melts at

0947-6539/02/0809-2014 $ 20.00+.50/0 *Chem. Eur. J.* **2002**, *8*, No. 9

Table 2. Thermal characterization of crown ether monodendrons.

Monodendron	Thermal transitions [°C] and corresponding enthalpy changes [kcal mol^{-1}][a]	
	Heating	Cooling
(3,4)12G1-B15C5	k[b] 81 (20.21) i[c] k 68 (15.52) i	i 47 (15.68) k
(4-3,4)12G1-B15C5	k 62 (7.75) − k 65 (0.78) k 73 (13.59) k 87 (1.14) i g 13 k 47 (0.57) S_A 54 (0.52) − k 55 (0.79) k 60 (2.99) i	i 50 (2.43) S_A[d] 43 (0.61) 6 g[e]
(4-3,4,5)12G1-B15C5	k 96 (19.30) i k 50 − k 66 (3.47) k 94 (15.9) i	i 34 (12.5) k
(3,4-3,4)12G2-B15C5	k 93 (4.09) − k 97 (3.25) k 112 (22.05) i − k 44 (0.73) k 111 (21.93) i	i 74 (1.20) k 61 (14.46) k
(3,4-3,5)12G2-B15C5	k 81 (25.01) i k 76 (21.20) i	i 41 (21.02) k
(4-3,4,5-3,5)12G2-B15C5	k 4 (6.18) k 82 (18.31) Φ_h[f] 103 (7.68) i k −21 (8.29) Φ_h 103 (8.13) i	i 87 (7.56) Φ_h −27 (5.91) k
(4-3,4,5-3,4,5)12G2-B15C5	k −20 (14.66) Φ_h 113 (2.46) i k −19 (12.37) Φ_h 113 (2.36) i	i 107 (2.51) Φ_h −24 (14.03) k
(3,4-3,4,5)12G2-B15C5	k 66 (21.66) − k 74 (3.14) k 92 (24.54) i k −12 (11.05) k 31 (1.01) k 71 (0.52) Cub 92 (0.13) i	i[g] 86 Cub[h] 58 (0.28) k 20 g −17 (8.88) k
(3,4,5-3,4,5)12G2-B15C5	k 60 (43.19) i k −13 (7.32) − k 39 (11.84) k 56 (12.33) i	i −18 (5.62) k
(4-3,4,5-3,4)12G2-B15C5	− k 26 (82.84) k 58 (54.78) k 112 (60.00) i k −24 (8.76) k 41 (0.44) Cub 91 (0.27) i	i 78 (0.14) Cub 40 (0.49) k −27 (2.54) k

[a] Data from the first heating and cooling scans are on the first line and data from the second heating are on the second line. [b] k = crystalline. [c] i = isotropic. [d] S_A = smectic A. [e] g = glassy. [f] Φ_h = *p6mm* hexagonal columnar lattice. [g] Observed by thermal optical polarized microscopy. [h] Cub = $Pm\bar{3}n$ cubic lattice.

Table 3. Thermal characterization of the selected complexes of crown ether monodendrons with NaOTf.

Monodendron · NaOTf [mol mol]	Thermal transitions [°C] and corresponding enthalpy changes [kcal mol^{-1}][a]	
	Heating	Cooling
(3,4)12G1-B15C5 · 0.8	k[b] 49 (10.23) Φ_h[c] 131 (0.14) i [d] S_B 33 (3.07) Φ_h 130 (0.19) i	i 126 (0.20) Φ_h 23 (2.84) S_B[e]
(4-3,4)12G1-B15C5 · 0.8	g[f] 19 k 23 (0.47) k 46 (0.28) S_A[g] 123 (0.11) i g 24 S_A 120 (0.31) i	i 117 (1.00) S_A 16 g
(4-3,4,5)12G1-B15C5 · 1.0	g 38 Φ_h 107 (0.51) i g 41 Φ_h 106 (0.24) i	i 98 (0.24) Φ_h 31 g
(3,4-3,4)12G2-B15C5 · 0.8	k 61 (19.37) Φ_h 143 (0.15) i g 31 Φ_h 143 (0.26) i	i 139 (0.21) Φ_h 27 g
(3,4-3,5)12G2-B15C5 · 0.9	k 56 (14.76) Φ_h 79 (0.26) i I g 23 Φ_h 79 (0.26) i	i 72 (0.28) Φ_h 19 g
(4-3,4,5-3,5)12G2-B15C5 · 0.8	k −23 (1.75) Φ_h 96 (3.77) i k −23 (3.67) Φ_h 94 (3.20) i	i 77 (3.77) Φ_h −28 (2.90) k
(4-3,4,5-3,4,5)12G2-B15C5 · 0.4	k −22 (11.61) k 54 (1.72) Φ_h 106 (0.55) i k −19 (8.99) Φ_h 104 (0.18) i	i 85 (0.54) Φ_h −25 (6.58) k
(3,4-3,4,5)12G2-B15C5 · 0.8	k 55 (18.61) Cub[h] 134 (0.20) i g 28 Cub 126 (0.09) i	i 113 (0.08) Cub
(3,4,5-3,4,5)12G2-B15C5 · 0.8	k 59 (43.46) i k −17 (7.47) g 27 Cub 90 (0.19) i	i −22 (7.84) k
(4-3,4,5-3,4)12G2-B15C5 · 0.4	g 28 Cub 117 (0.29) i g 27 Cub 117 (0.64) i	i 115 (0.06) Cub −26 (3.39) k

[a] Data from the first heating and cooling scans are on the first line and data from the second heating are on the second line. [b] k = crystalline. [c] Φ_h = *p6mm* hexagonal columnar lattice. [d] i = isotropic. [e] S_B = smectic B. [f] g = glassy. [g] S_A = smectic A. [h] Cub = $Pm\bar{3}n$ cubic lattice.

54 °C. Increasing the amount of NaOTf in the complex from 0.2 mol mol^{-1} to 1.0 mol mol^{-1} increases the transition from isotropic to Φ_h phase from 40 to 136 °C. However, this complexation process does not influence the temperature transition from the Φ_h to the S_B phase. Within instrumental error the Φ_h to S_B and S_B to Φ_h transition temperatures are constant. This suggests that the complexation of **(3,4)12G1-B15C5** with NaOTf disrupts its crystallization to *uncover* most probably its virtual S_B phase.[10] Therefore, the S_B phase is not induced or affected by complexation with NaOTf. Nevertheless, the creation of the Φ_h phase of **(3,4)12G1-B15C5** is induced by the ionic interactions generated by the ionization of NaOTf due to its complexation by the **B15C5** part of the monodendron.

A second example of monodendritic crown ether is provided by **(4-3,4)12G1-B15C5** and its complexes with NaOTf (Figure 3). On cooling **(4-3,4)12G1-B15C5** forms a S_A phase followed by crystallization. On reheating, the crystal phase melts in the S_A phase which undergoes isotropization. Above this isotropization, a new crystallization process occurs followed by melting at 60 °C. Complexation with NaOTf suppresses first the highest crystalline phase of **(4-3,4)12G1-**

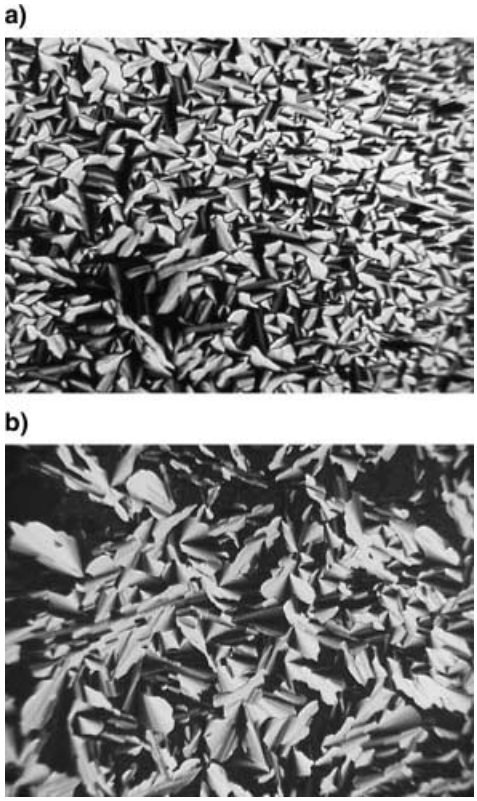

Figure 1. Representative optical polarized texture exhibited by a) **(4-3,4)12G1-B15C5 · NaOTf** (1:0.8) obtained upon cooling from 123 to 115 °C with 1 °C min^{-1} (smectic A, S_A) and b) **(3,4-3,5)12G2-B15C5 · NaOTf** (1:0.6) obtained upon cooling from 79 to 51 °C with 1 °C min^{-1} (*p6mm* hexagonal columnar lattice, Φ_h).

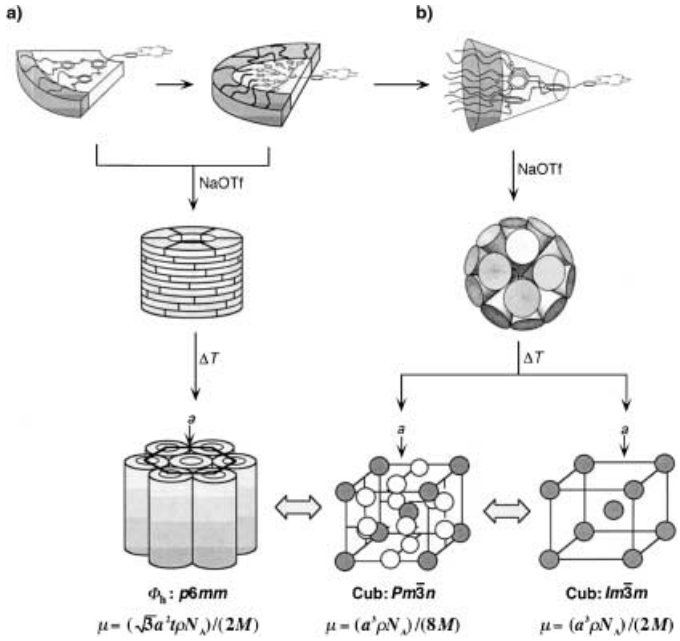

Scheme 3. Schematic representation of a) the self-assembly of building blocks based on flat tapered and disc-shaped monodendrons into supramolecular cylindrical dendrimers and their subsequent self-organization in a *p6mm* hexagonal columnar (Φ_h) lattice and b) the self-assembly of the conical monodendrons into supramolecular spherical dendrimers and their subsequent self-organization in $Pm\bar{3}n$ and $Im\bar{3}m$ cubic (Cub) lattices. For explanation on the calculation of μ, see Table 5.

B15C5 and subsequently the crystalline phase which is present below the S_A phase. Simultaneously the S_A-isotropic phase transition temperature increases. **(4-3,4)12G1-B15C5 · NaOTf** = 0.5 to 1.0 exhibit only the S_A phase above the glass transition temperature. Therefore, the stability of the S_A-phase of **(4-3,4)12G1-B15C5** is enhanced by complexation. By contrast, the S_B phase of **(3,4)12G1-B15C5** is not affected by complexation (Figure 2). These two different mechanisms will be discussed based on the structures of the two smectic phases as determined by XRD experiments.

The third representative example is provided by **(3,4-3,4)12G2-B15C5** and its complexes with NaOTf (Figure 4). **(3,4-3,4)12G2-B15C5** is crystalline. Complexation with NaOTf destabilizes the crystalline phase and stabilizes the newly formed Φ_h phase of this compound to the point that the **(3,4-3,4)12G2-B15C5/NaOTf** = 1.2 exhibits an enantiotropic Φ_h phase starting from its glass transition temperature (37 °C) up to the isotropization temperature (173 °C). This is a remarkable trend.

A similar trend is observed in the case of **(3,4-3,5)12G2-B15C5** and its complexes with NaOTf (not shown here). **(3,4-3,5)12G2-B15C5** is crystalline. Complexation with NaOTf decreases its crystallization tendency and stabilizes the formation of the Φ_h phase. **(3,4-3,5)12G2-B15C5 · NaOTf** = 1.0 exhibits a Φ_h phase from glass transition (23 °C) up to 90 °C. All the experiments have demonstrated the stabilization of the Φ_h phase through complexation with NaOTf. In all these cases the shape of the dendritic monodendron is tapered, that is, it represents a fragment of disc that is smaller than half of a disc (Scheme 3).

Therefore, the next question is what is the influence of complexation on the self-assembly of a dendritic crown ether that has a shape identical to half of a disc (Scheme 3). The answer to this question is provided by the investigation of **(4-3,4,5-3,5)12G2-B15C5** and **(4-3,4,5-3,4,5)12G2-B15C5** and of their complexes with NaOTf (Scheme 4). Both **(4-3,4,5-3,5)12G2-B15C5** and **(4-3,4,5-3,4,5)12G2-B15C5** are the first examples of monodendritic crown ethers that self-assemble in the absence of complexation. Previous examples were provided only by semifluorinated compounds.[2e] **(4-3,4,5-3,5)12G2-B15C5** forms a Φ_h phase that is stable from −21 up to 103 °C while **(4-3,4,5-3,4,5)12G2-B15C5** a Φ_h phase that is stable from −19 to 113 °C. Figure 5 shows the DSC traces of the present dendritic crown ethers and the complexation experiments for the **(4-3,4,5-3,5)12G2-B15C5 · NaOTf** series of experiments. The corresponding complexes for the **(4-3,4,5-3,4,5)12G2-B15C5 · NaOTf** follow the same trend and therefore, are not shown. The DSC traces shown in Figure 5 follow a completely different trend from the one exhibited by the tapered monodendrons. The Φ_h phase derived from tapered monodendrons undergoes a dramatic stabilization through complexation, while the Φ_h phase generated from half-disc monodendrons is destabilized upon complexation. The stability of the Φ_h phase of **(4-3,4,5-3,5)12G2-B15C5** decreases from 103 to 94 °C upon complexation with up to 0.8 mol NaOTf (Figure 5). The same trend is shown by the complexes of **(4-3,4,5-3,4,5)12G2-B15C5**. The stability of their Φ_h phase decreases (not shown) from 113 to 104 °C upon complexation with up to 0.4 mol NaOTf.

  0947-6539/02/0809-2016 $ 20.00+.50/0 *Chem. Eur. J.* **2002**, *8*, No. 9

Table 4. Measured *d*-spacings of the intermediary and crown ether monodendrons.

Monodendrons	*T* [°C]	NaOTf [equiv]	Lattice	d_{001}[a] d_{100} d_{320} [Å]	d_{002}[a] d_{110} d_{321} [Å]	d_{003}[a] d_{200} d_{400} [Å]	d_{004}[a] d_{210} d_{420} [Å]	d_{005}[a] d_{211} d_{421} [Å]	d_{006}[a] d_{220} d_{332} [Å]	d_{310} d_{432} [Å]	d_{222} [Å]
(3,4)12G1-B15C5	20	0.8	S_B[a]		30.9	20.6	15.4	12.4	10.3		
	70	0.8	*p6mm*	45.0		22.5					
(4-3,4)12G1-CO_2CH_3	57		*p6mm*	49.7	28.9	24.9					
(4-3,4)12G1-CO_2H	77		*p6mm*	46.6							
(4-3,4)12G1-B15C5	40	0.8	S_A[a]	66.1	33.0						
	120	0.8	S_A[a]	53.3	26.6						
(4-3,4,5)12G1-CO_2H	87		*p6mm*	35.4		17.7					
(4-3,4,5)12G1-B15C5	66	0.6	*p6mm*	49.0	28.1	25.1					
(3,4-3,4)12G2-CO_2H	112		$Pm\bar{3}n$			42.4	37.7	34.2	29.6	26.7	
					22.6	21.1	18.8	18.3			
(3,4-3,4)12G2-B15C5	80	0.8	*p6mm*	54.6	31.5	27.3	20.6				
	110	0.8	*p6mm*	51.9	30.0	26.0	19.5				
(3,4-3,5)12G2-CO_2H	66		*p6mm*	38.0	21.5	18.6					
(3,4-3,5)12G2-B15C5	75	0.9	*p6mm*	45.3	26.3	22.8					
(4-3,4,5-3,5)12G2-CO_2CH_3	60		*p6mm*	40.5		20.4					
(4-3,4,5-3,5)12G2-CO_2H	80		$Im\bar{3}m$		38.5	27.2		22.1	19.1		
(4-3,4,5-3,5)12G2-B15C5	100	0.0	*p6mm*	39.0	22.6	19.6					
(4-3,4,5-3,4,5)12G2-CO_2CH_3	70		*p6mm*	41.7	23.7	20.5					
(4-3,4,5-3,4,5)12G2-CO_2H	140		$Im\bar{3}m$		37.2	26.3		21.5	18.6		
(4-3,4,5-3,4,5)12G2-B15C5	20	0.0	*p6mm*	38.4	22.1	19.0					
	70	0.0	*p6mm*	37.6	21.6	18.7					
	105	0.0	*p6mm*	36.9	21.3	18.5					
(3,4-3,4,5)12G2-CH_2OH	80		$Pm\bar{3}n$		58.0	41.5	37.3	34.0	29.6	26.4	24.3
				23.3	22.5	20.9	18.6	18.2	17.8		
(3,4-3,4,5)12G2-B15C5	95	0.8	$Pm\bar{3}n$			56.4	50.5	46.2	40.1	35.8	
				31.3	30.2	28.3	25.2	24.6			
	120	0.8	$Pm\bar{3}n$		77.5	54.7	49.0	44.8	38.8	34.7	
				30.4	29.3	27.4	24.4	23.9			
(3,4,5-3,4,5)12G2-CO_2H	105		$Pm\bar{3}n$		48.8	34.5	30.9	28.3	23.7	21.3	
					18.2	17.0					
(3,4,5-3,4,5)12G2-B15C5	68	0.8	$Pm\bar{3}n$			48.4	43.4	39.6	34.3	30.6	
				26.8	25.9	24.2					
(4-3,4,5-3,4)12G2-CO_2CH_3	112		$Pm\bar{3}n$			49.1	43.8	40.1	34.8	31.2	28.5
				27.4	26.5	24.9	22.2	21.7			
(4-3,4,5-3,4)12G2-CO_2H	140		$Pm\bar{3}n$			45.8	40.9	37.6	32.5	29.1	26.6
				25.7	24.8	23.2	20.6	20.2			
(4-3,4,5-3,4)12G2-B15C5	90	0.0	$Pm\bar{3}n$			57.8	51.7	47.3	41.0	36.6	33.4
				32.1	30.9	28.9	25.9	25.2		21.4	
	105	0.4	$Pm\bar{3}n$			58.7	52.6	48.0	41.6	37.2	33.9
				32.6	31.4	29.4	26.3	25.6			

[a] d_{001}, d_{002}, d_{003}, d_{004}, d_{005} and d_{006} refer to S_A and S_B phases.

The final question refers to the influence of complexation on the formation of $Pm\bar{3}n$ cubic phases generated from spherical supramolecular dendrimers. Spherical supramolecular dendrimers are self-assembled from various fragments of spheres[2n, 3b] including conic shapes (Scheme 3). Three examples were investigated so far with conic monodendritic crown ethers (Scheme 4) and they all follow the same trend. Complexation with NaOTf enhances the stability of a monotropic and enantiotropic cubic phase and produces an enantiotropic cubic phase of much higher thermal stability. A single example is elaborated in Figure 6. **(3,4-3,4,5)12G2-B15C5** shows a narrow monotropic phase (first DSC scan not shown). Complexation with NaOTf destabilizes its crystalline phase and increases the isotropization temperature from 92 to 126 °C for the **(3,4-3,4,5)12G2-B15C5 · NaOTf** = 0.8.

Correlation between the molecular structure of the monodendrons, the functionality at their focal point and the structure of supramolecular dendrimers: A schematic summary of the series of experiments reported in this manuscript is presented in Scheme 4. This Scheme provides the following sequence of information: the shape of the monodendron containing a non-interacting -CO_2CH_3 or H-bonding -CO_2H or -CH_2OH at the focal point, followed by the change in shape that occurs by the incorporation of the **B15C5** at the focal point and the influence of complexation with NaOTf on the self-assembly process. This sequence of events can be most easily followed by the sets of arrows from the right side of each dendron. The first important message that comes from Scheme 4 is that the functionality at the focal point of the monodendron determines its self-assembly capability. **(4-3,4)12G1-CO_2CH_3**, **(4-3,4,5-3,5)12G2-CO_2CH_3**, and **(4-3,4,5-3,4,5)12G2-CO_2CH_3** exhibit tapered and half-disc shapes, respectively and subsequently self-assemble in columnar supramolecular dendrimers. **(3,4,5-3,4,5)12G2-CO_2CH_3** and **(4-3,4,5-3,4)12G2-CO_2CH_3** display conic shapes and self-

Table 5. Structural characterization of supramolecular dendrimers self-assembled from intermediary and crown ether monodendrons.

Monodendron	T [°C]	NaOTf [equiv]	Lattice	$\langle d_{100}\rangle$[a] [Å]	a [Å]	ρ_{20}[d] [g cm^{-3}]	D [Å]	μ'[i]	μ	α'[m] [°]
(3,4)12G1-B15C5	20	0.8	S_B			1.10	61.8[e]			
	70	0.8	*p6mm*	45.0	52.0[a]	1.10	52.0[f]		10[j]	36.0
(4-3,4)12G1-CO_2CH_3	57		*p6mm*	49.9	57.6[a]	1.05	57.6[f]		12[j]	30.0
(4-3,4)12G1-CO_2H	77		*p6mm*	46.6	53.8[a]	1.04	53.8[f]		11[j]	32.7
(4-3,4)12G1-B15C5	40	0.8	S_A			1.11	66.1[e]			
	120	0.8	S_A			1.11	53.3[e]			
(4-3,4,5)12G1-CO_2H	87		*p6mm*	35.4	40.9[a]	1.02	40.9[f]		4[j]	90.0
(4-3,4,5)12G1-B15C5	66	0.6	*p6mm*	49.3	56.9[a]	1.09	56.9[f]		7[j]	32.9
(3,4-3,4)12G2-CO_2H	112		$Pm\bar{3}n$		83.5[b]	1.02	51.8[g]	334	42[k]	8.6
(3,4-3,4)12G2-B15C5	80	0.8	*p6mm*	54.6	63.0[a]	1.10	63.0[f]		8[j]	45.0
	110	0.8	*p6mm*	51.9	59.9[a]	1.10	59.9[f]		7[j]	51.4
(3,4-3,5)12G2-CO_2H	66		*p6mm*	37.5	43.3[a]	1.02	43.3[f]		4[j]	90.0
(3,4-3,5)12G2-B15C5	75	0.9	*p6mm*	45.5	52.5[a]	1.09	52.5[f]		6[j]	60.0
(4-3,4,5-3,5)12G2-CO_2CH_3	60		*p6mm*	40.7	47.0[a]	1.02	47.0[f]		3[j]	120.0
(4-3,4,5-3,5)12G2-CO_2H	80		$Im\bar{3}m$		54.2[c]	1.03	53.4[h]	48	24[l]	15.0
(4-3,4,5-3,5)12G2-B15C5	100	0.0	*p6mm*	39.1	45.2[a]	1.10	45.2[f]		2[j]	180.0
(4-3,4,5-3,4,5)12G2-CO_2CH_3	70		*p6mm*	41.2	47.6[a]	1.02	47.6[f]		2[j]	180.0
(4-3,4,5-3,4,5)12G2-CO_2H	140		$Im\bar{3}m$		52.6[c]	1.03	51.8[h]	30	15[l]	24
(4-3,4,5-3,4,5)12G2-B15C5	20	0.0	*p6mm*	38.2	44.1[a]	1.11	44.1[f]		2[j]	180.0
	70	0.0	*p6mm*	37.5	43.3[a]	1.11	43.3[f]		2[j]	180.0
	105	0.0	*p6mm*	36.9	42.6[a]	1.11	42.6[f]		2[j]	180.0
(3,4-3,4,5)12G2-CH_2OH	80		$Pm\bar{3}n$		83.5[b]	1.00	51.8[g]	228	28[k]	12.9
(3,4-3,4,5)12G2-B15C5	95	0.8	$Pm\bar{3}n$		113.0[b]	1.09	70.1[g]	519	65[k]	5.5
	120	0.8	$Pm\bar{3}n$		109.5[b]	1.09	67.9[g]	472	59[k]	6.1
(3,4,5-3,4,5)12G2-CO_2H	105		$Pm\bar{3}n$		68.3[b]	1.04	42.4[g]	96	12[k]	30.0
(3,4,5-3,4,5)12G2-B15C5	68	0.8	$Pm\bar{3}n$		96.8[b]	1.08	60.1[g]	248	31[k]	11.6
(4-3,4,5-3,4)12G2-CO_2CH_3	112		$Pm\bar{3}n$		98.7[b]	1.03	61.2[g]	285	36[k]	10.0
(4-3,4,5-3,4)12G2-CO_2H	140		$Pm\bar{3}n$		92.2[b]	1.03	57.2[g]	234	29[k]	12.4
(4-3,4,5-3,4)12G2-B15C5	90	0.0	$Pm\bar{3}n$		115.7[b]	1.09	71.8[g]	431	54[k]	6.7
	105	0.4	$Pm\bar{3}n$		117.5[b]	1.11	72.9[g]	460	58[k]	6.2

[a] *p6mm* hexagonal columnar lattice parameter $a = 2\langle d_{100}\rangle/\sqrt{3}$; $\langle d_{100}\rangle = (d_{100}+\sqrt{3}d_{110}+\sqrt{4}d_{200}+\sqrt{7}d_{210})/4$. [b] $Pm\bar{3}n$ cubic lattice parameter $a = (\sqrt{2}d_{110}+\sqrt{4}d_{200}+\sqrt{5}d_{210}+\sqrt{6}d_{211}+\sqrt{8}d_{220}+\sqrt{10}d_{310}+\sqrt{12}d_{222}+\sqrt{13}d_{320}+\sqrt{14}d_{321}+\sqrt{16}d_{400}+\sqrt{20}d_{420}+\sqrt{21}d_{421}+\sqrt{22}d_{332}+\sqrt{29}d_{432})/14$. [c] $Im\bar{3}m$ cubic lattice parameter $a = (\sqrt{2}d_{110}+\sqrt{4}d_{200}+\sqrt{6}d_{211}+\sqrt{8}d_{220})/4$. [d] ρ_{20} = experimental density at 20 °C. [e] D = layer spacing. [f] Experimental column diameter $D = 2\langle d_{100}\rangle/\sqrt{3}$. [g] Experimental $Pm\bar{3}n$ spherical diameter $D = 2^3\sqrt{3a^3/32\pi}$. [h] Experimental $Im\bar{3}m$ spherical diameter $D = 2^3\sqrt{3a^3/8\pi}$. [i] Number of monodendrons per unit cell $\mu' = (a^3 N_A \rho)/M$. [j] Number of monodendrons per 4.7 Å column stratum $\mu = (\sqrt{3}N_A D^2 t\rho)/2M$ (Avogadro's number $N_A = 6.022045\times10^{23}$ mol^{-1}, the average height of the column stratum $t = 4.7$ Å, and M = molecular weight of monodendron). [k] Number of monodendrons per $Pm\bar{3}n$ spherical dendrimer $\mu = \mu'/8$. [l] Number of monodendrons per $Im\bar{3}m$ spherical dendrimer $\mu = \mu'/2$. [m] Projection of the solid angle for tapered and conical monodendron $\alpha' = 360/\mu$ [°].

assemble in spherical supramolecular dendrimers, respectively. All other monodendrons which contain CO_2CH_3 groups at the focal point are crystalline. However, the replacement of -CO_2CH_3 from the focal point of the dendron with an hydrogen-bonding group such as -CO_2H or -CH_2OH transforms all compounds into self-assembling monodendrons. Exception is **(3,4)12G1-CO_2H** which remains crystalline. It is interesting to observe that while the transition from **(4-3,4)12G1-CO_2CH_3** to **(4-3,4)12G1-CO_2H** maintains a tapered shape for the monodendron, the transition from **(4-3,4,5-3,5)12G2-X** and **(4-3,4,5-3,4,5)12G2-X** with X = CO_2CH_3 to CO_2H changes the shape of the monodendron from half-disc to conic. The insertion of the crown ether (CE) at the focal point replaces the hydrogen-bonding capability of the parent CO_2H group and therefore, most of the dendritic crown ethers adopt a similar shape to that of the monodendrons containing the CO_2CH_3 group at the focal point. A significant exception is provided by **(4-3,4)12G1-B15C5** which adopts a parallelepiped rather than a tapered shape and therefore forms a S_A phase. This is because the **B15C5** is bulkier than the -CO_2CH_3 group and therefore makes the dendron more symmetric.

The NaOTf complexation experiments already described can be now explained in a more quantitative way. In all cases complexation destabilizes the crystalline phase of the monodendritic crown ether since the binding process changes the shape of the crown ether. The tapered monodendrons with X = -CO_2CH_3, -CO_2H or -CH_2OH which have a larger planar solid angle α'[2j, m, n] such as **(4-3,4,5)12G1-CO_2H** and **(3,4-3,5)12G2-CO_2H** ($\alpha' = 90.0°$ in both cases) maintain a tapered shape after functionalization with **B15C5** and complexation with NaOTf. However, their tapered shape has, as expected, a lower α' (i.e., $\alpha' = 32.9$ and 60.0°). Tapered monodendrons with lower α' (**(4-3,4)12G1-CO_2CH_3** with $\alpha' = 30.0°$ and **(4-3,4)12G1-CO_2H** with $\alpha' = 32.7°$) change, as expected, after functionalization with **B15C5** and complexation their shape into parallelepiped. Conic monodendrons with small α' such as **(3,4-3,4)12G2-CO_2H** ($\alpha' = 8.6°$), **(3,4,5-3,5)12G2-CO_2H** ($\alpha' = 15°$) and **(4-3,4,5-3,4,5)12G2-CO_2H** ($\alpha' = 24°$) change their shape after functionalization with **B15C5** and complexation or in the absence of complexation from conic into tapered. Finally, conic monodendrons with larger α', that is, **(3,4-3,4,5)12G2-CH_2OH** ($\alpha' = 12.9°$), **(3,4,5-3,4,5)12G2-COOH** ($\alpha' = 30.0°$) and **(4-3,4,5-3,4)12G2-X** with X = CO_2CH_3

0947-6539/02/0809-2018 $ 20.00+.50/0 *Chem. Eur. J.* **2002**, *8*, No. 9

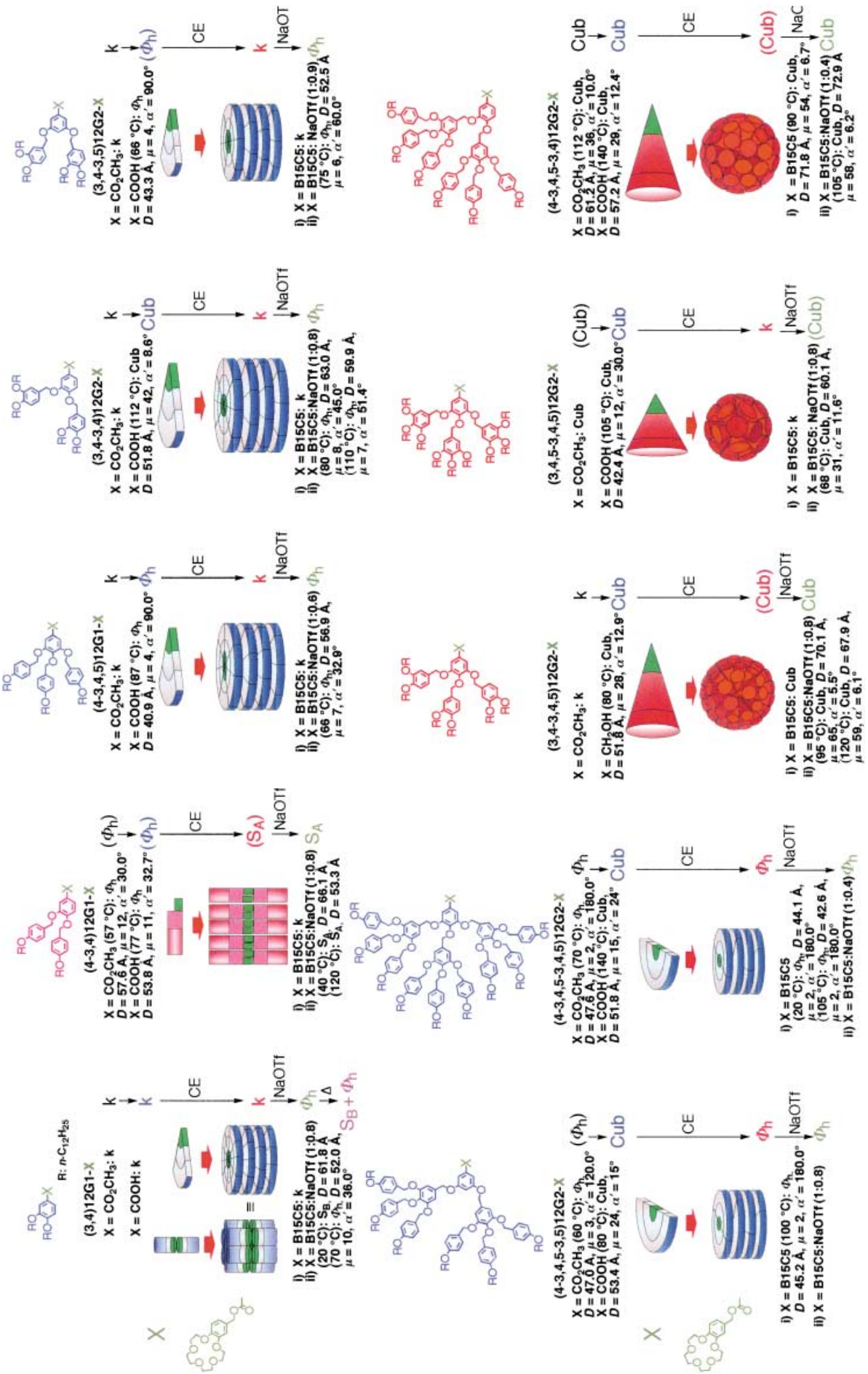

Scheme 4. Retrostructural analysis of supramolecular dendrimers self-assembled from dendritic crown ethers (CE).

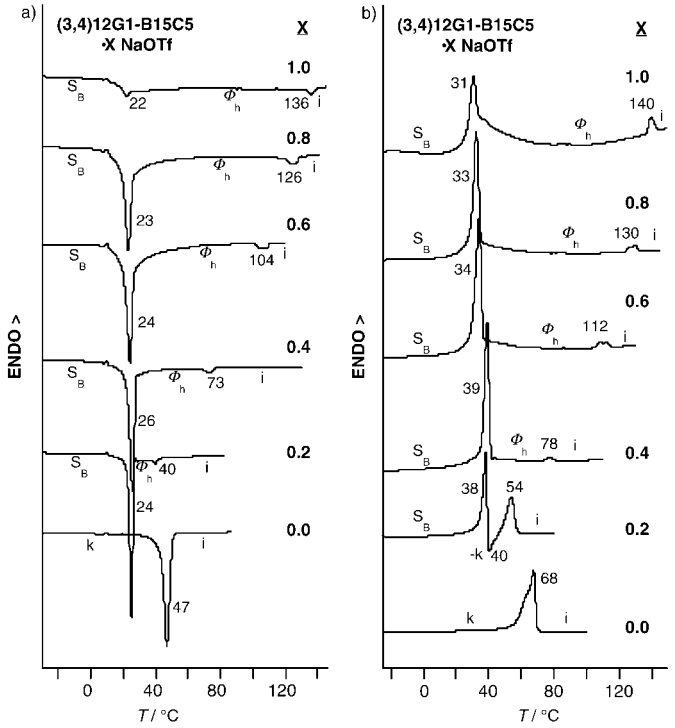

Figure 2. DSC traces ($10\,^{\circ}C\,min^{-1}$) of the complexes of **(3,4)12G1-B15C5** with NaOTf recorded during: a) first cooling scan and b) second heating scan.

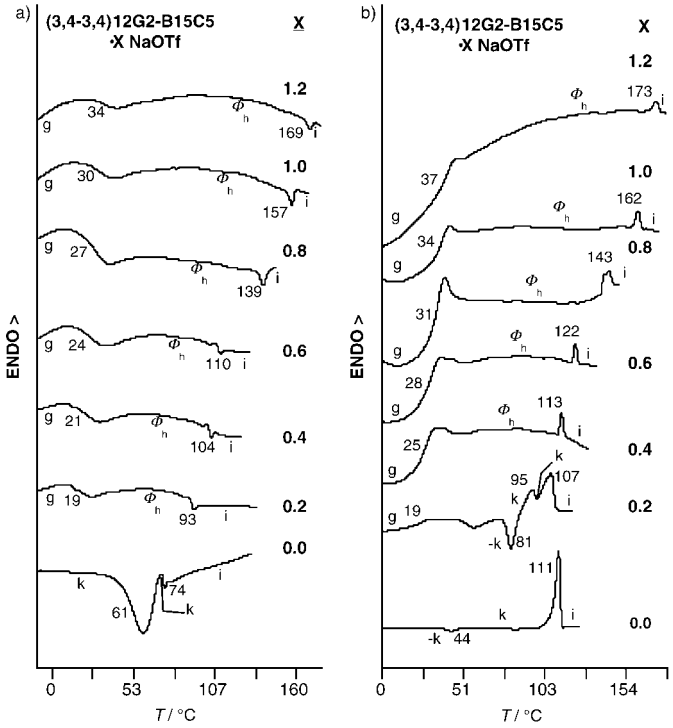

Figure 4. DSC traces ($10\,^{\circ}C\,min^{-1}$) of the complexes of **(3,4-3,4)12G2-B15C5** with NaOTf recorded during: a) first cooling scan and b) second heating scan.

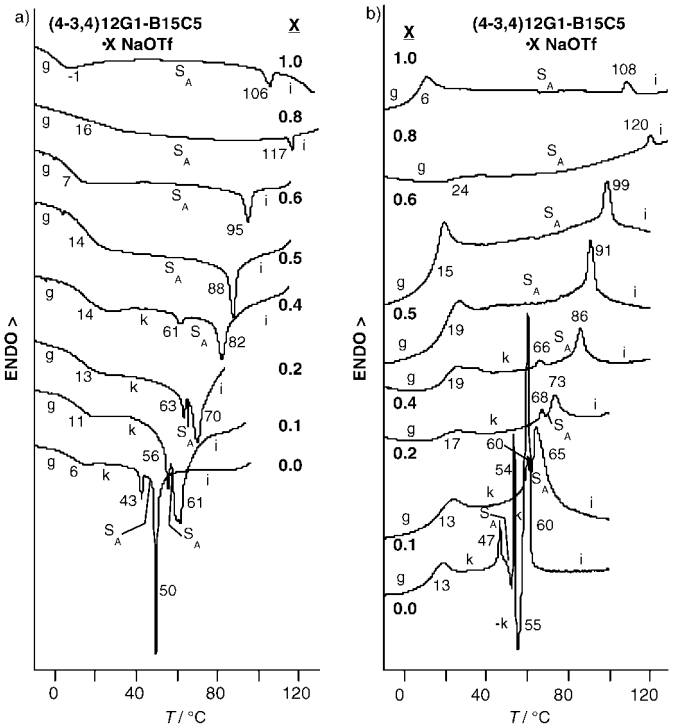

Figure 3. DSC traces ($10\,^{\circ}C\,min^{-1}$) of the complexes of **(4-3,4)12G1-B15C5** with NaOTf recorded during: a) first cooling scan and b) second heating scan.

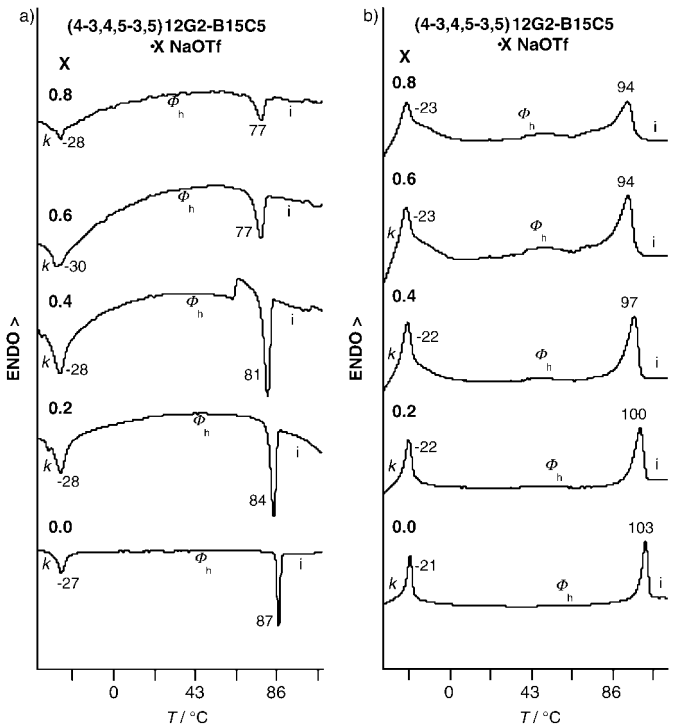

Figure 5. DSC traces ($10\,^{\circ}C\,min^{-1}$) of the complexes of **(4-3,4,5-3,5)12G2-B15C5** with NaOTf recorded during: a) first cooling scan and b) second heating scan.

($\alpha' = 10.0\,^{\circ}$) and X = CO_2H ($\alpha' = 12.4\,^{\circ}$) maintain a conic shape after functionalization with **B15C5**.

Complexation with NaOTf provides the following five different trends: a) stabilizes the $Pm\bar{3}n$ cubic phase self-organized from spherical supramolecular dendrimers which are self-assembled from conic monodendrons; b) stabilizes the S_A phase generated from parallelepiped monodendrons; c) has no effect on the stability of the S_B phase generated from

0947-6539/02/0809-2020 $ 20.00+.50/0 *Chem. Eur. J.* **2002**, *8*, No. 9

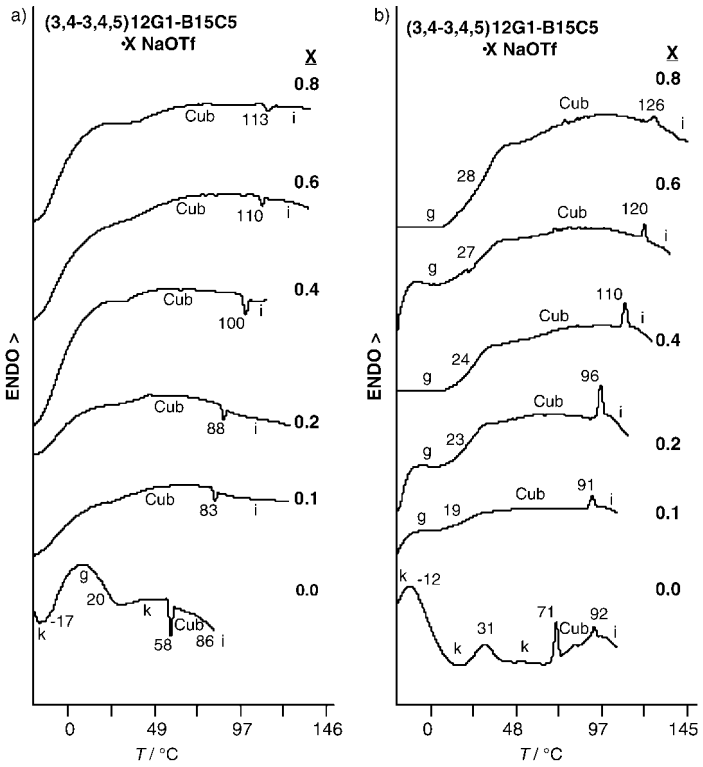

Figure 6. DSC traces ($10\,^{\circ}C\,min^{-1}$) of the complexes of **(3,4-3,4,5)12G2-B15C5** with NaOTf recorded during: a) first cooling scan and b) second heating scan.

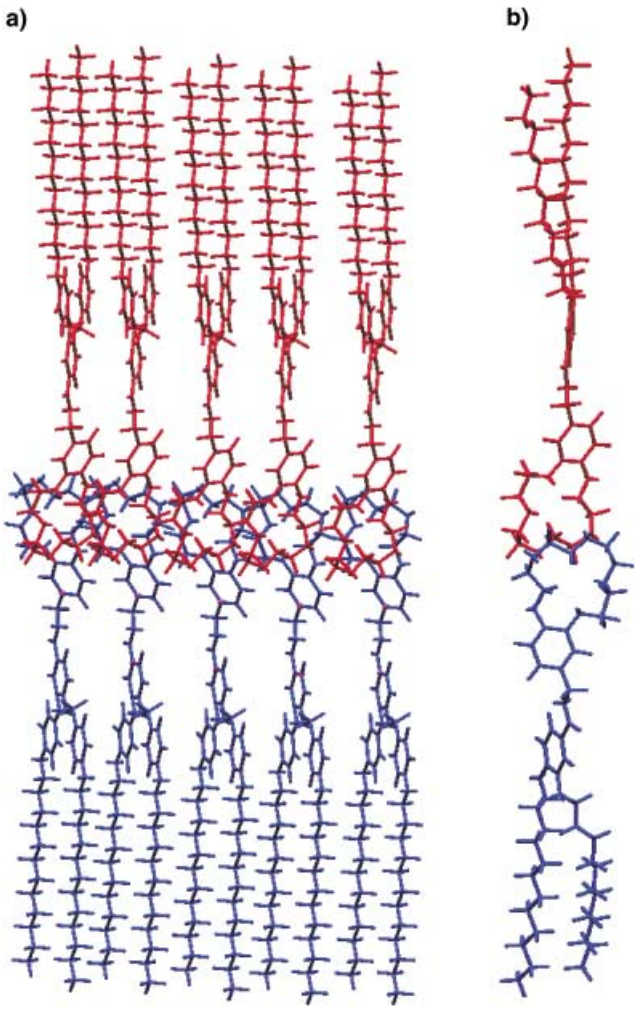

Figure 7. Molecular models of the smectic layers of a) smectic A (S_A) and b) smectic B (S_B) phases.

parallelepiped monodendrons; d) stabilizes the *p6mm* hexagonal columnar phase self-organized from cylindrical supramolecular dendrimers which are self-assembled from tapered monodendrons; and e) destabilizes the *p6mm* hexagonal columnar phase self-organized from cylindrical supramolecular dendrimers self-assembled from half-disc monodendrons.

We will try to provide explanations for these trends. In the case a) the conic monodendron contains the crown ether at their apex and upon self-assembly into supramolecular spherical dendrimers the crown ethers are placed at the center of the sphere. When NaOTf is ionized in the center of the supramolecular sphere the ionic interaction created enhances the stability of the supramolecular object and of its cubic lattice. In case b), the S_A phase has a bilayer interdigitated structure (Figure 7a) in which the **B15C5** units are facing each other in the center of the bilayer. Again complexation can easily explain the enhanced stability of the S_A phase since the placement of the **B15C5** can enhance after complexation the interdendritic interactions. Case c) is observed for the S_B phase. No enhanced stability of the S_B phase is observed upon complexation since no interaction between the non-interdigitated bilayer structures shown in Figure 8b is possible. Cases d) and e) can be explained by the creation of an ion channel that penetrates through the center of the column.[2a, b, e] This ion channel seems to be most effective when the dendritic crown ether has a tapered shape. However, when the shape of the dendritic crown ether is equivalent to half of a disc, complexation with NaOTf destabilizes the formation of the ion channel (case e). More structural experiments are required to elucidate the difference between cases d) and e). It is, however, rewarding to conclude that the influence of complexation with NaOTf resembles that of the dependence of polymerization from the field of liquid crystalline polymers[10] known as the "polymer effect" and therefore this trend should be considered a "supramolecular polymer effect".[11] Unrelated examples of mediation of supramolecular structure by a combination of crown ethers or other ligands and ionic interactions are actively exploited also in other laboratories.[12] Dendritic crown ethers that do not self-assemble were recently reported by Gitsov and Ivanova.[13] Nevertheless, the monodendritic crown ethers and their complexes with NaOTf reported here provide the largest diversity of liquid crystalline phases encountered so far in any library of supramolecular dendrimers reported from our[2–5] and other laboratories.[14]

Conclusion

The synthesis of the benzyl ether based self-assembling monodendrons containing benzo[15]crown-5 at their focal point is described. These dendritic building blocks self-assemble and subsequently self-organize either spontaneously

or after complexation with NaOTf into smectic B, smectic A, *p6mm* hexagonal columnar (Φ_h) and $Pm\bar{3}n$ cubic lattices. The dependence between the shape of the monodendron, the shape of the supramolecular dendrimer, the symmetry of the supramolecular lattice obtained by its spontaneous self-assembly and self-organization and the influence of complexation with NaOTf on the stability of various supramolecular lattices were elucidated by retrostructural analysis of the lattices generated from supramolecular dendrimers. A very delicate dependence between the shape of the dendritic crown ether and the stability of its supramolecular lattice obtained by complexation with NaOTf was demonstrated and mechanisms of complexation mediated self-assembly were suggested. These mechanisms many help to elaborate novel ionactive supramolecular concepts.

Experimental Section

Materials: 1,3-Dicyclohexylcarbodiimide (DCC, 99%), 4-(dimethylamino)pyridine (DMAP, 99%) (from Aldrich), *p*-toluenesulfonic acid (98%), KOH, acetone, THF, and EtOH (from Fisher, ACS reagent) were used as received. CH_2Cl_2 (from Fisher, ACS reagent) was dried over CaH_2 and freshly distilled before use. The materials used in the synthesis of intermediary compounds reported previously were identical to those reported in the previous publications.

Techniques: ^{1}H NMR (200 MHz) and ^{13}C NMR (50 MHz) spectra were recorded on a Varian Gemini 200 spectrometer at 20 °C with tetramethylsilane (TMS) as internal standard. The purity of products was determined by a combination of thin-layer chromatography (TLC) on silica gel plates (Kodak) with fluorescent indicator and high pressure liquid chromatography (HPLC) using a Perkin–Elmer Series10 high-pressure liquid chromatograph equipped with an LC-100 column oven and Nelson Analytical 900 series integrator data station. THF was used as solvent at an oven temperature of 40 °C. Detection was by UV absorbance at 254 nm. Thermal transitions were measured on a Perkin–Elmer DSC-7 differential scanning calorimetry (DSC) equipped with a TADS data station. In all cases, the heating and cooling rates were 10 °C min^{-1}. First-order transition temperatures were reported as the maxima and minima of their endothermic and exothermic peaks. The glass transition temperatures (T_g) were read at the middle of the change in heat capacity. Indium and zinc were used as calibration standards. An Olympus BX-40 thermal optical polarized microscope (TOPM) (100× magnification) equipped with a Mettler FP 82 hot stage and a Mettler FP80 central processor was used to observe thermal transitions and verify the anisotropic and isotropic textures. X-ray diffraction (XRD) experiments on liquid crystal phases were performed by using either a helium-filled flat plate wide angle (WAXS) camera or a pinhole-collimated small angle (SAXS) camera, and also by using an Image Plate area detector (MAR Research) with a graphite-monochromatized a pinhole-collimator beam and a helium tent. The samples, in glass capillaries, were held in a temperature-controlled cell (±0.1 °C). Ni-filtered $Cu_{K\alpha}$ radiation was used. Experiments were also performed at several small-angle stations of the Synchrotron Radiation Source at Daresbury (UK). A double-focused beam and a quadrant detector were used. In both cases, the sample was held in a capillary within a custom-built temperature cell controlled to within ±0.1 °C. Densities (ρ_{20}) were determined by flotation in gradient columns at 20 °C. Elemental analysis of all new compounds (M-H-W Laboratories, Phoenix, AZ) agrees with the calculated value within less than ±0.4%.

Macromodel 6.0 from Columbia Innovation Corp. was used on a Silicon Graphics Indy workstation to model the arrangement of smectic A and smectic B phases.

Synthesis: The syntheses of 4′-hydroxymethylbenzo[15]crown-5 (**B15C5**),[2a] 4-dimethylaminopyridinium *p*-toluenesulfonate (DPTS),[2a] NaOTf,[2a] methyl 3,4-bis(*n*-dodecan-1-yloxy)benzoate [**(3,4)12G1-CO$_2$CH$_3$**],[6] 3,4-bis(*n*-dodecan-1-yloxy)benzoic acid [**(3,4)12G1-CO$_2$H**],[7] methyl 3,4-bis[*p*-(*n*-dodecan-1-yloxy)benzyloxy]benzoate [**(4-3,4)12G1-CO$_2$CH$_3$**],[3b] 3,4-bis[*p*-(*n*-dodecan-1-yloxy)benzyloxy]benzoic acid [**(4-3,4)12G1-CO$_2$H**],[3b] methyl 3,4,5-tris[*p*-(*n*-dodecan-1-yloxy)benzyloxy]-benzoate [**(4-3,4,5)12G1-CO$_2$CH$_3$**],[8] 3,4,5-tris[*p*-(*n*-dodecan-1-yloxy)benzyloxy]benzoic acid [**(4-3,4,5)12G1-CO$_2$H**],[2h, 8] methyl 3,4-bis[3′,4′-bis(*n*-dodecan-1-yloxy)benzyloxy]benzoate [**(3,4-3,4)12G2-CO$_2$CH$_3$**],[3b] 3,4-bis[3′,4′-bis(*n*-dodecan-1-yloxy)benzyloxy]benzoic acid [**(3,4-3,4)12G2-CO$_2$H**],[3b] methyl 3,5-bis[3′,4′-bis(*n*-dodecan-1-yloxy)benzyloxy]benzoate [**(3,4-3,5)12G2-CO$_2$CH$_3$**],[3b] 3,5-bis[3′,4′-bis(*n*-dodecan-1-yloxy)benzyloxy]-benzoic acid [**(3,4-3,5)12G2-CO$_2$H**],[3b] methyl 3,5-bis{3′,4′,5′-tris-[*p*-(*n*-dodecan-1-yloxy)benzyloxy]benzyloxy}benzoate [**(4-3,4,5-3,5)12G2-CO$_2$CH$_3$**],[2n] 3,5-bis{3′,4′,5′-tris[*p*-(*n*-dodecan-1-yloxy)benzyloxy]benzyloxy}-benzoic acid [**(4-3,4,5-3,5)12G2-CO$_2$H**],[2n] methyl 3,4,5-tris{3′,4′,5′-tris[*p*-(*n*-dodecan-1-yloxy)benzyloxy]benzyloxy}benzoate [**(4-3,4,5-3,4,5)12G2-CO$_2$CH$_3$**],[2h] methyl 3,4,5-tris[3′,4′-bis(*n*-dodecan-1-yloxy)benzyloxy]benzoate [**(3,4-3,4,5)12G2-CO$_2$CH$_3$**],[3b] 3,4,5-tris[3′,4′-bis(*n*-dodecan-1-yloxy)-benzyloxy]benzoic acid [**(3,4-3,4,5)12G2-CO$_2$H**],[3b] methyl 3,4,5-tris[3′,4′,5′-tris(*n*-dodecan-1-yloxy)benzyloxy]benzoic acid [**(3,4,5-3,4,5)-12G2-CO$_2$CH$_3$**],[2f] 3,4,5-tris[3′,4′,5′-tris(*n*-dodecan-1-yloxy)benzyloxy]benzoic acid [**(3,4,5-3,4,5)12G2-CO$_2$H**],[2f] methyl 3,4-bis{3′,4′,5′-tris[*p*-(*n*-dodecan-1-yloxy)benzyloxy]benzyloxy}benzoate [**(4-3,4,5-3,4)12G2-CO$_2$CH$_3$**],[2n] 3,4-bis{3′,4′,5′-tris[*p*-(*n*-dodecan-1-yloxy)benzyloxy]benzyloxy}-benzoic acid [**(4-3,4,5-3,4)12G2-CO$_2$H**][2n] and 4′-methylbenzo[15]crown-5 3,4,5-tris[*p*-(*n*-dodecan-1-yloxy)benzyloxy]benzoate [**(4-3,4,5)12G1-B15C5**],[2a] have been reported previously.

3,4,5-Tris{3′,4′,5′-tris[*p*-(*n*-dodecan-1-yloxy)benzyloxy]benzyloxy}benzoic acid [(4-3,4,5-3,4,5)12G2-CO$_2$H]: In a 200 mL one-neck round bottom flask equipped with a reflux condenser, **(4-3,4,5-3,4,5)12G2-CO$_2$CH$_3$** (2.0 g, 0.65 mmol) and KOH (0.26 g, 4.6 mmol) in a mixture of 95% EtOH (30 mL) and THF (50 mL) were heated gently under reflux until the reaction was completed (3 h as determined by TLC and ^{1}H NMR. After cooling to room temperature, the solvent was distilled under reduced pressure with the solid residue taken up in THF (30 mL). The solution was acidified with 50% aqueous CH_3COOH and the resulting mixture was precipitated by the addition of cold H_2O (200 mL) and the product filtered off. Recrystallization from acetone/CH_2Cl_2 (1:1, 80 mL) yielded a white solid (1.67 g, 83.9%). Thermal transitions and corresponding enthalpy changes are reported in Table 1. Purity (HPLC), 99+ %; TLC (CH_2Cl_2): $R_f = 0$; ^{1}H NMR ($CDCl_3$, TMS): $\delta = 0.89$ (t, 27H, $J = 6.6$ Hz, CH_3), 1.27 (m, 162H, $CH_3(CH_2)_9$), 1.72 (m, 18H, CH_2CH_2OAr), 3.84–3.92 (m, 18H, CH_2CH_2OAr), 4.70 (brs, 6H, ArCH_2OAr, 4-(3′,4′,5′)-positions), 4.80 (s, 4H, ArCH_2OAr, 3,5-(4′)-positions), 4.86 (s, 8H, ArCH_2OAr, 3,5-(3′,5′)-positions), 5.00 (brs, 6H, ArCH_2OAr, 3,4,5-positions), 6.70–6.77 (m, 22H, Ar*H meta* to CH_2OAr, 3,4,5-(3′,4′,5′), Ar*H ortho* to CH_2OAr, 3,5-positions), 7.13–7.27 (m, 20H, Ar*H ortho* to CH_2OAr, 3,4,5-(3′,5′), Ar*H ortho* to CH_2OAr, 4-position), 7.51 (s, 2H, Ar*H ortho* to COOH); ^{13}C NMR ($CDCl_3$, TMS): $\delta = 14.1$ (*C*H_3), 22.7 (CH_3CH_2), 26.1 ($CH_2CH_2CH_2OAr$), 29.3 ($CH_3(CH_2)_2CH_2$), 29.6 ($CH_3(CH_2)_3(CH_2)_5$), 31.9 ($CH_3CH_2CH_2$), 67.9 (CH_2CH_2OAr), 70.9 (Ar*C*H_2OAr, 3,4,5-(3′,5′)-positions), 71.5 (Ar*C*H_2-OAr, 3,5-positions), 74.5 (Ar*C*H_2OAr, 3,4,5-(4′)-positions), 74.7 (Ar*C*H_2-OAr, 4-positions), 106.6–107.2 (Ar*C ortho* to CH_2OAr, 3,4,5-positions), 109.7 (Ar*C ortho* to COOH), 114.2–114.9 (Ar*C meta* to CH_2OAr, 3,4,5-(3′,4′,5′)-positions), 123.7 (Ar*C ipso* to COOH), 128.8–129.8 (Ar*C ortho* to CH_2OAr and Ar*C ipso* to CH_2OAr, 3,4,5-(3′,4′,5′)-positions), 132.1–132.9 (Ar*C para* to CH_2OAr, 3,4,5-positions), 138.3 (Ar*C ipso* to CH_2OAr, 3,4,5-positions), 142.2 (Ar*C para* to COOH), 152.6 (Ar*C meta* to COOH), 153.2 (Ar*C meta* to CH_2OAr, 3,4,5-positions), 158.9 (Ar*C para* to CH_2OAr, 3,4,5-(3′,4′,5′)-positions), 171.0 (*C*OOH); elemental analysis calcd (%) for $C_{199}H_{294}O_{23}$: C 78.25, H 9.70; found: C 78.30, H 9.59.

General procedure for the synthesis of monodendrons containing B15C5: The monodendrons containing crown ether at their focal points were synthesized by estherification with the corresponding benzoic acids and 4′-hydroxymethylbenzo[15]crown-5 in the presence of DCC and catalyzed by DPTS in CH_2Cl_2.

4′-Methylbenzo[15]crown-5 3,4-bis(*n*-dodecan-1-yloxy)benzoate [(3,4)12G1-B15C5]: **(3,4)12G1-CO$_2$H** (1.1 g, 2.2 mmol), 4′-hydroxymethylbenzo-[15]crown-5 (0.80 g, 2.7 mmol), and DPTS (0.21 g, 0.67 mmol) were dissolved in CH_2Cl_2 (50 mL). DCC (0.69 g, 3.4 mmol) was added and then the mixture was heated under reflux. After 24 h, the reaction mixture was passed through a glass fiber filter and evaporated in vacuo. Purification by flash column chromatography (silica gel, CH_2Cl_2) and recrystallization from acetone (30 mL) gave **(3,4)12G1-B15C5** as a white product (0.83 g,

0947-6539/02/0809-2022 $ 20.00+.50/0 *Chem. Eur. J.* **2002**, *8*, No. 9

48%). Thermal transitions and corresponding enthalpy changes are reported in Table 2. Purity (HPLC), 99+%; TLC (hexane/EtOAc 4:1): $R_f = 0$; ^{1}H NMR ($CDCl_3$, TMS): $\delta = 0.88$ (t, 6H, $J = 6.7$ Hz, CH_3), 1.27 (m, 36H, $CH_3(CH_2)_9$), 1.83 (m, 4H, CH_2CH$_2$OAr), 3.76 (s, 8H, (OCH_2CH_2)$_2$), 3.91 (m, 4H, ArOCH$_2$CH_2O), 4.03 (m, 4H, CH_2OAr), 5.24 (s, 2H, CO$_2$CH_2Ar), 6.86–6.97 (m, 4H, Ar*H* (5) *meta* to CO$_2$CH$_2$Ar, Ar*H meta* to CH$_2$, Ar*H ortho* to CH$_2$), 7.55 (d, 1H, $J = 2.0$ Hz, Ar*H* (2) *ortho* to CO$_2$CH$_2$Ar, 2-position), 7.65 (s, 1H, Ar*H* (6) *ortho* to CO$_2$CH$_2$Ar); ^{13}C NMR ($CDCl_3$, TMS): $\delta = 14.1$ (*C*H$_3$), 22.7 (*C*H$_2$CH$_3$), 26.0–29.6 ((*C*H$_2$)$_8$), 31.9 (*C*H$_2$CH$_2$CH$_3$), 66.5 (CO$_2$*C*H$_2$Ar), 69.0 (CH$_2$*C*H$_2$OAr), 69.1, 69.3, 69.6, 70.5, 71.1 (crown ether), 111.9 (Ar*C* (5) *meta* to CO$_2$CH$_2$Ar), 113.8 (*ortho* to CH$_2$ and O on crown ether), 114.4 (Ar*C* (2) *ortho* to CO$_2$CH$_2$Ar), 114.5 (*meta* to CH$_2$ on crown ether), 121.7 (Ar*C ortho* to CH$_2$ on crown ether), 122.4 (Ar*C ipso* to CO$_2$CH$_2$Ar), 123.7 (Ar*C* (6) *ortho* to CO$_2$CH$_2$Ar), 129.4 (Ar*C ipso* to CH$_2$ on crown ether), 148.5 (Ar*C* (3) *meta* to CO$_2$CH$_3$, 3-position), 149.2 (Ar*C ipso* to O on crown ether), 153.3 (Ar*C para* to CO$_2$CH$_2$Ar), 166.4 (*C*O$_2$CH$_2$Ar); elemental analysis calcd (%) for $C_{46}H_{74}O_9$: C 71.65, H 9.67; found: C 71.68, H 9.62.

4′-Methylbenzo[15]crown-5 3,4-bis[*p*-(*n*-dodecan-1-yloxy)benzyloxy]benzoate [(4-3,4)12G1-B15C5]: **(4-3,4)12G1-CO$_2$H** (1.4 g, 2.0 mmol), 4′-hydroxymethylbenzo[15]crown-5 (0.68 g, 2.3 mmol), DPTS (0.12 g, 0.40 mmol), and DCC (0.49 g, 2.4 mmol) were dissolved in CH_2Cl_2 (20 mL) at reflux and heated (18 h). Purification by flash column chromatography (silica gel, CH_2Cl_2) and recrystallization from acetone (40 mL) gave compound (1.28 g, 65.4%) as a white solid. Thermal transitions and corresponding enthalpy changes are reported in Table 2. Purity (HPLC), 99+%; TLC (hexane/EtOAc 20:1): $R_f = 0$; ^{1}H NMR ($CDCl_3$, TMS): $\delta = 0.88$ (t, 6H, $J = 6.5$ Hz, CH_3), 1.26 (m, 36H, $CH_3(CH_2)_9$), 1.78 (m, 4H, CH_2CH$_2$OAr), 3.76 (s, 8H, (OCH_2CH_2)$_2$), 3.89–3.97 (m, 8H, CH$_2$CH_2OAr, ArOCH$_2$CH_2O), 4.15 (m, 4H, ArOCH_2-CH$_2$O), 5.08 (s, 2H, ArCH_2OAr, 4-position), 5.12 (s, 2H, ArCH_2OAr, 3-position), 5.22 (s, 2H, CO$_2$CH_2Ar), 6.84–6.99 (m, 8H, Ar*H meta* to CH$_2$OAr, 3,4-positions, Ar*H* (5) *meta* to CO$_2$CH$_2$Ar, Ar*H meta* to CH$_2$, Ar*H ortho* to CH$_2$), 7.32–7.36 (m, 4H, Ar*H ortho* to CH$_2$OAr, 3,4-positions), 7.61–7.65 (m, 2H, Ar*H ortho* to CO$_2$CH$_2$Ar); ^{13}C NMR ($CDCl_3$, TMS): $\delta = 14.1$ (*C*H$_3$), 22.7 (*C*H$_2$CH$_3$), 26.0–29.6 ((*C*H$_2$)$_8$), 31.9 (*C*H$_2$CH$_2$CH$_3$), 66.5 (CO$_2$*C*H$_2$Ar), 68.0 (CH$_2$*C*H$_2$OAr), 69.1, 69.6, 70.5, 70.7 (crown ether), 71.1 (Ar*C*H$_2$OAr), 113.4 (Ar*C ortho* to CH$_2$ and O on crown ether), 113.8 (Ar*C* (5) *meta* to CO$_2$CH$_2$Ar), 114.5 (Ar*C meta* to CH$_2$OAr, 3,4-positions, Ar*C meta* to CH$_2$ on crown ether), 115.8 (Ar*C* (2) *ortho* to CO$_2$CH$_2$Ar), 121.7 (Ar*C ortho* to CH$_2$ on crown ether), 122.9 (Ar*C ipso* to CO$_2$CH$_2$Ar), 124.3 (Ar*C* (6) *ortho* to CO$_2$CH$_2$Ar), 128.6 (Ar*C ipso* CH$_2$CO$_2$Ar), 128.8–129.1 (Ar*C ortho* to CH$_2$OAr, 3,4-positions, Ar*C ipso* CH$_2$OAr, 3,4-positions), 148.4–149.2 (Ar*C* (3) *meta* CO$_2$CH$_2$Ar, Ar*C ipso* O on crown ether), 153.1 (Ar*C para* to CO$_2$CH$_2$Ar), 159.0 (Ar*C para* to CH$_2$OAr, 3,4-positions), 166.0 (*C*O$_2$CH$_2$Ar); elemental analysis calcd (%) for $C_{60}H_{86}O_{11}$: C 73.29, H 8.82; found: C 73.32, H 8.77.

4′-Methylbenzo[15]crown-5 3,4-bis[3′,4′-bis(*n*-dodecan-1-yloxy)benzyloxy]benzoate [(3,4-3,4)12G2-B15C5]: **(3,4-3,4)12G2-CO$_2$H** (1.50 g, 1.40 mmol), 4′-hydroxymethylbenzo[15]crown-5 (0.50 g, 1.7 mmol), DPTS (0.13 g, 0.42 mmol), and DCC (0.43 g, 2.1 mmol) were dissolved in CH_2Cl_2 (30 mL) and heated under reflux for 16 h. A white solid compound (1.20 g, 63.5%) was obtained after flash column chromatography (silica gel, CH_2Cl_2) and recrystallization from a mixture of CH_2Cl_2 and acetone (2:1, 25 mL). Thermal transitions and corresponding enthalpy changes are reported in Table 2. Purity (HPLC), 99+%; TLC (THF): $R_f = 0.71$; ^{1}H NMR ($CDCl_3$, TMS): $\delta = 0.89$ (t, 12H, $J = 6.8$ Hz, CH_3), 1.27 (m, 72H, $CH_3(CH_2)_9$), 1.75 (m, 8H, CH_2CH$_2$OAr), 3.77 (s, 8H, (OCH_2CH_2)$_2$), 3.90–4.01 (m, 12H, CH$_2$CH_2OAr, ArOCH$_2$CH_2O), 4.16 (m, 4H, ArOCH_2-CH$_2$O), 5.08 (s, 2H, ArCH_2OAr, 4-position), 5.11 (s, 2H, ArCH_2OAr, 3-position), 5.24 (s, 2H, CO$_2$CH_2Ar), 6.81–7.00 (m, 10H, Ar*H* to CH$_2$OAr, 3,4-positions, Ar*H* (5) *meta* to CO$_2$CH$_2$Ar, Ar*H meta* to CH$_2$, Ar*H ortho* to CH$_2$), 7.62–7.67 (overlapped peaks, 2H, Ar*H ortho* to CO$_2$CH$_2$Ar); ^{13}C NMR ($CDCl_3$, TMS): $\delta = 14.0$ (*C*H$_3$), 22.6 (*C*H$_2$CH$_3$), 26.0–30.5 ((*C*H$_2$)$_8$), 31.9 (*C*H$_2$CH$_2$CH$_3$), 66.4 (CO$_2$*C*H$_2$Ar), 69.1 (CH$_2$CH$_2$OAr), 69.3, 69.5, 70.5, 70.8 (crown ether), 71.2 (Ar*C*H$_2$OAr), 113.1 (Ar*C ortho* to CH$_2$ and O on crown ether), 113.2 (Ar*C* (2′) *ortho* to CH$_2$OAr, 3,4-positions), 113.6 (Ar*C* (5′) *meta* to CH$_2$OAr, 3,4-positions), 113.8 (Ar*C* (5) *meta* to CO$_2$CH$_2$OAr), 114.5 (Ar*C meta* to CH$_2$CO$_2$Ar on crown ether), 115.6 (Ar*C* (2) *ortho* to CO$_2$CH$_2$Ar), 119.9–120.1 (Ar*C ortho* (6′) to CH$_2$OAr, 3,4-positions), 121.6 (Ar*C ortho* to CH$_2$CO$_2$Ar on crown ether), 122.9 (Ar*C ipso* to CO$_2$CH$_2$Ar), 124.0 (Ar*C* (6) *ortho* to CO$_2$CH$_2$Ar), 129.0 (Ar*C ipso* to CH$_2$CO$_2$Ar on crown ether), 129.3 (Ar*C ipso* CH$_2$OAr, 3,4-positions), 148.3 (Ar*C* (2) *meta* to CO$_2$CH$_2$Ar), 148.9–149.2 (Ar*C para* to CH$_2$OAr, 3,4-positions, Ar*C* (3′) *meta* to CH$_2$OAr, 3,4-positions, Ar*C ipso* O on crown ether), 153.0 (Ar*C para* to CO$_2$CH$_2$Ar), 166.0 (*C*O$_2$CH$_2$Ar); elemental analysis calcd (%) for $C_{84}H_{134}O_{13}$: C 74.63, H 9.99; found: C 74.64, H 9.95.

4′-Methylbenzo[15]crown-5 3,5-bis[3′,4′-bis(*n*-dodecan-1-yloxy)benzyloxy]benzoate [(3,4-3,5)12G2-B15C5]: **(3,4-3,5)12G2-CO$_2$H** (1.4 g, 1.3 mmol), 4′-hydroxymethylbenzo[15]crown-5 (0.45 g, 1.5 mmol), DPTS (82 mg, 0.26 mmol), and DCC (0.32 g, 1.6 mmol) were taken up in CH_2Cl_2 (20 mL) at room temperature for 12 h. After flash column chromatography (silica gel, CH_2Cl_2) and recrystallization from acetone (30 mL) a white crystal (1.46 g, 82.7%) was obtained. Thermal transitions and corresponding enthalpy changes are reported in Table 2. Purity (HPLC), 99+%; TLC (THF): $R_f = 0.59$; ^{1}H NMR ($CDCl_3$, TMS): $\delta = 0.88$ (t, 12H, $J = 5.9$ Hz, CH_3), 1.26 (m, 72H, $CH_3(CH_2)_9$), 1.78 (m, 8H, CH_2CH$_2$OAr), 3.75 (s, 8H, (OCH_2CH_2)$_2$), 3.92–4.02 (m, 12H, CH$_2$CH_2OAr, ArOCH$_2$CH_2O), 4.15 (m, 4H, ArOCH_2CH$_2$O), 4.94 (s, 4H, ArCH_2OAr, 3,5-positions), 5.25 (s, 2H, CO$_2$CH_2Ar), 6.78 (t, 1H, $J = 2.4$ Hz, Ar*H para* to CO$_2$CH$_2$Ar), 6.84–7.01 (m, 9H, Ar*H* to CH$_2$OAr, 3,5-positions, Ar*H meta* to CH$_2$, Ar*H ortho* to CH$_2$), 7.29 (d, 2H, $J = 2.1$ Hz, Ar*H ortho* to CO$_2$CH$_2$Ar); ^{13}C NMR ($CDCl_3$, TMS): $\delta = 13.9$ (*C*H$_3$), 22.5 (*C*H$_2$CH$_3$), 25.9–29.5 ((*C*H$_2$)$_8$), 31.8 (*C*H$_2$CH$_2$CH$_3$), 66.7 (CO$_2$*C*H$_2$Ar), 69.0 (crown ether), 69.1 (CH$_2$*C*H$_2$OAr), 69.4 (crown ether), 70.2 (Ar*C*H$_2$OAr), 70.4, 70.9 (crown ether), 107.0 (Ar*C para* to CO$_2$CH$_2$Ar), 108.3 (Ar*C ortho* to CO$_2$CH$_2$Ar), 113.5–113.6 (Ar*C* (2′) *ortho* to CH$_2$OAr, 3,5-positions, Ar*C* (5′) *meta* to CH$_2$OAr, 3,5-positions, Ar*C ortho* to CH$_2$ and O on crown ether), 114.5 (Ar*C meta* to CH$_2$ on crown ether), 120.4 (Ar*C* (6′) *ortho* to CH$_2$OAr, 3,5-positions), 121.6 (Ar*C ortho* to CH$_2$ on crown ether), 128.8 (Ar*C ipso* to CH$_2$OAr, 3,5-positions, Ar*C ipso* to CH$_2$CO$_2$Ar on crown ether), 144.0 (Ar*C ipso* to CO$_2$CH$_2$Ar), 149.0 (Ar*C para* to CH$_2$OAr, 3,5-positions), 149.2 (Ar*C* (3′) *meta* to CH$_2$OAr, 3,5-positions), 160.0 (Ar*C meta* to CO$_2$CH$_2$Ar), 166.1 (*C*O$_2$CH$_2$Ar); elemental analysis calcd (%) for $C_{84}H_{134}O_{13}$: C 74.63, H 9.99; found: C 74.59, H 9.94.

4′-Methylbenzo[15]crown-5 3,4,5-tris[3′,4′-bis(*n*-dodecan-1-yloxy)benzyloxy] benzoate [(3,4-3,4,5)12G2-B15C5]: From **(3,4-3,4,5)12G2-CO$_2$H** (1.4 g, 0.91 mmol) and 4′-hydroxymethylbenzo[15]crown-5 (0.31 g, 1.0 mmol) in the presence of DPTS (57 mg, 0.18 mmol) and DCC (0.224 g, 1.09 mmol) in CH_2Cl_2 (20 mL) at room temperature (reaction time, 16 h), a white crystal (1.13 g, 68.3%) was obtained after flash column chromatography (silica gel, CH_2Cl_2) and recrystallization from CH_2Cl_2 and acetone (1:3, 30 mL). Thermal transitions and corresponding enthalpy changes are reported in Table 2. Purity (HPLC), 99+%; TLC (THF): $R_f = 0.81$; ^{1}H NMR ($CDCl_3$, TMS): $\delta = 0.89$ (t, 18H, $J = 6.9$ Hz, CH_3), 1.27 (m, 108H, $CH_3(CH_2)_9$), 1.79 (m, 12H, CH_2CH$_2$OAr), 3.72–3.77 (m, 10H, CH_2OAr, 4-(3′)-position, (OCH_2CH_2)$_2$), 3.93–4.02 (m, 14H, CH_2OAr, 3,5-(3′,4′)- and 4-(4′)-positions, ArOCH$_2$CH_2O), 4.17 (m, 4H, ArOCH_2CH$_2$O), 5.03 (s, 6H, ArCH_2OAr, 3,4,5-positions), 5.25 (s, 2H, CO$_2$CH_2Ar), 6.74–6.99 (m, 12H, Ar*H* to CH$_2$OAr, 3,4,5-positions, Ar*H meta* to CH$_2$, Ar*H ortho* to CH$_2$), 7.40 (s, 2H, Ar*H ortho* to CO$_2$CH$_2$Ar); ^{13}C NMR ($CDCl_3$, TMS): $\delta = 14.1$ (*C*H$_3$), 22.7 (*C*H$_2$CH$_3$), 26.1–30.2 ((*C*H$_2$)$_8$), 31.9 (*C*H$_2$CH$_2$CH$_3$), 66.8 (CO$_2$*C*H$_2$Ar), 69.1 (crown ether), 69.3 (CH$_2$*C*H$_2$OAr), 69.6, 70.4, 70.5 (crown ether), 71.1 (ArCH$_2$OAr), 108.5 (Ar*C ortho* to CO$_2$CH$_2$Ar), 113.7 (Ar*C ortho* to CH$_2$ and O on crown ether), 113.8 (Ar*C* (2′) *ortho* to CH$_2$OAr, 3,4,5-positions), 114.6 (Ar*C* (5′) *meta* to CH$_2$OAr, 3,4,5-positions, Ar*C meta* to CH$_2$ on crown ether), 120.6 (Ar*C* (6′) *ortho* to CH$_2$OAr, 3,4,5-positions), 121.8 (Ar*C ortho* to CH$_2$ on crown ether), 124.1 (Ar*C ipso* to CO$_2$CH$_2$Ar), 129.0 (Ar*C ipso* to CH$_2$OAr, 3,4,5-positions, Ar*C ipso* to CH$_2$CO$_2$Ar on crown ether), 144.2 (Ar*C para* to CO$_2$CH$_2$Ar), 149.1–149.4 (Ar*C* (3′) *meta* to CH$_2$OAr, 3,4,5-positions, Ar*C para* to CH$_2$OAr, 3,4,5-positions), 153.8 (Ar*C meta* to CO$_2$CH$_2$Ar), 166.2 (*C*O$_2$CH$_2$Ar); elemental analysis calcd (%) for $C_{115}H_{188}O_{16}$: C 75.61, H 10.37; found: C 75.59, H 10.33.

4′-Methylbenzo[15]crown-5 3,4,5-tris[3′,4′,5-tris(*n*-dodecan-1-yloxy)benzyloxy]benzoate [(3,4,5-3,4,5)12G2-B15C5]: **(3,4,5-3,4,5)12G2-CO$_2$H** (1.5 g, 0.72 mmol), 4′-hydroxymethylbenzo[15]crown-5 (0.26 g, 0.86 mmol), DPTS (67 mg, 0.22 mmol), and DCC (0.22 g, 1.1 mmol) were heated to reflux in CH_2Cl_2 (40 mL) for 18 h. After purification by column chromatography [silica gel, CH_2Cl_2 to CH_2Cl_2/MeOH 20:1] and recrystallization from a mixture of CH_2Cl_2 and acetone (1:1, 30 mL) gave **(3,4,5-3,4,5)12G2-**

B15C5 (1.14 g, 67.1 %) as a white solid. Thermal transitions and corresponding enthalpy changes are reported in Table 2. Purity (HPLC), 99 + %; TLC (THF): $R_f = 0.91$; ^{1}H NMR ($CDCl_3$, TMS): $\delta = 0.88$ (t, 27 H, $J =$ 6.6 Hz, $CH_3(CH_2)_{11}$), 1.26 (m, 162 H, $CH_3(CH_2)_8$), 1.74 (m, 18 H, CH_2CH_2OAr), 3.71 – 3.76 (m, 12 H, CH_2OAr, 4-(3′,5′)-positions, $(OCH_2CH_2)_2$), 3.84 – 3.96 (m, 18 H, CH_2CH_2OAr, 3,5-(3′,5′)-positions, 3,4,5-(4′)-positions, $ArOCH_2CH_2O$), 4.17 (m, 4 H, $ArOCH_2CH_2O$), 5.02 (s, 6 H, $ArCH_2OAr$, 3,4,5-positions), 5.25 (s, 2 H, CO_2CH_2Ar), 6.59 (s, 2 H, Ar*H ortho* to CH_2OAr, 4-position), 6.63 (s, 4 H, Ar*H ortho* to CH_2OAr, 3,5-positions), 6.89 (d, 1 H, $J = 8.8$ Hz, Ar*H meta* to CH_2), 6.99 (m, 2 H, Ar*H ortho* to CH_2), 7.40 (s, 2 H, Ar*H ortho* to CO_2CH_2Ar); ^{13}C NMR ($CDCl_3$, TMS): $\delta = 14.0$ (CH_3), 22.6 (CH_3CH_2), 26.1 – 30.5 ($(CH_2)_8$), 31.9 ($CH_3CH_2CH_2$), 66.7 (CO_2CH_2Ar), 68.8 (crown ether), 69.0 (CH_2CH_2OAr, 3,4,5-(3′,5′)-positions), 69.5, 70.5, 71.0 (crown ether), 71.6 ($ArCH_2OAr$, 3,5-positions), 73.3 (CH_2CH_2OAr, 3,4,5-(4′)-positions), 75.1 ($ArCH_2OAr$, 4-position), 105.7 (Ar*C ortho* to CH_2OAr, 3,5-positions), 106.1 (Ar*C ortho* to CH_2OAr, 4-position), 109.7 (Ar*C ortho* to CO_2CH_2Ar), 113.8 (Ar*C ortho* to CH_2 and O on crown ether), 114.5 (Ar*C meta* to CH_2 on crown ether), 121.6 (Ar*C ortho* to CH_2CO_2Ar on crown ether), 125.2 (Ar*C ipso* to CO_2CH_2Ar), 129.0 (Ar*C ipso* to CH_2CO_2Ar on crown ether), 131.6 (Ar*C para* to CH_2OAr, 3,5-positions), 132.3 (Ar*C para* to CH_2OAr, 4-position), 137.8 (Ar*C ipso* to CH_2OAr, 3,4,5-positions), 143.4 (Ar*C para* to CO_2CH_2Ar), 149.2 (Ar*C ipso* O on crown ether), 152.1 (Ar*C meta* to CO_2CH_2Ar), 153.0 (Ar*C meta* to CH_2OAr, 4-position), 153.2 (Ar*C meta* to CH_2OAr, 3,5-positions), 166.0 (CO_2CH_2Ar); elemental analysis calcd (%) for $C_{151}H_{260}O_{19}$: C 76.21, H 11.01; found: C 76.18, H 11.03.

4′-Methylbenzo[15]crown-5 3,4-bis{3′,4′,5′-tris[*p*-(*n*-dodecan-1-yloxy)benzyloxy]benzyloxy}benzoate [(4-3,4,5-3,4)12G2-B15C5]: **(4-3,4,5-3,4)12G2-CO_2H** (1.5 g, 0.72 mmol), 4′-hydroxymethylbenzo[15]crown-5 (0.26 g, 0.87 mmol) in the presence of DPTS (68 mg, 0.22 mmol) and DCC (0.22 g, 1.1 mmol) were stirred in CH_2Cl_2 (40 mL) at room temperature for 12 h. Purification by flash column chromatography with gradient elution [silica gel, CH_2Cl_2/MeOH 20:1 to CH_2Cl_2/MeOH 10:1] and recrystallization from CH_2Cl_2 and acetone (2:1, 30 mL) gave **(4-3,4,5-3,4)12G2-B15C5** (0.98 g, 58 %) as a white solid. Thermal transitions and corresponding enthalpy changes are reported in Table 2. Purity (HPLC), 99 + %. TLC (THF): $R_f = 0.81$; ^{1}H NMR ($CDCl_3$, TMS): $\delta = 0.89$ (t, 18 H, $J = 6.9$ Hz, CH_3), 1.27 (m, 108 H, $CH_3(CH_2)_9$), 1.77 (m, 12 H, CH_2CH_2OAr), 3.76 (s, 8 H, $(OCH_2CH_2)_2$), 3.87 – 3.93 (m, 16 H, CH_2CH_2OAr, $ArOCH_2CH_2O$), 4.12 (m, 4 H, $ArOCH_2CH_2O$), 4.84 (s, 4 H, $ArCH_2OAr$, 3,4-(4′)-positions), 4.94 (s, 8 H, $ArCH_2OAr$, 3,4-(3′,5′)-positions), 5.08 (s, 4 H, $ArCH_2OAr$, 3,4-positions), 5.25 (s, 2 H, CO_2CH_2Ar), 6.72 – 6.87 (m, 18 H, Ar*H meta* to CH_2OAr, 3,4-(3′,4′,5′)-positions, Ar*H ortho* to CH_2OAr, 3,4-positions, Ar*H meta* to CO_2CH_2Ar, 5-position, Ar*H meta* to CH_2), 6.99 (m, 2 H, Ar*H ortho* to CH_2), 7.22 – 7.26 (m, 12 H, Ar*H ortho* to CH_2OAr, 3,4-(3′,4′,5′)-positions), 7.69 (m, 2 H, Ar*H ortho* to CO_2CH_2Ar); ^{13}C NMR ($CDCl_3$, TMS): $\delta = 14.1$ (CH_3), 22.6 (CH_2CH_3), 26.1 ($CH_2CH_2CH_2OAr$), 29.3 ($CH_3(CH_2)_2CH_2$), 29.6 ($CH_3(CH_2)_3(CH_2)_5$), 30.1 (CH_2CH_2OAr), 31.9 ($CH_3CH_2CH_2$), 66.5 (CO_2CH_2Ar), 67.9 (CH_2CH_2OAr, 3,4-[3′,4′,5′-(4″)] positions), 69.0, 69.1, 69.5, 70.5 (crown ether), 71.0 – 71.4 ($ArCH_2OAr$, 3,4-(3′,5′)-positions, 3,4-positions), 74.7 ($ArCH_2OAr$, 3,4-(4′)-positions), 106.9 (Ar*C ortho* to CH_2OAr, 3-position), 107.1 (Ar*C ortho* to CH_2OAr, 4-position), 113.4 (Ar*C* (5) *meta* to CO_2CH_2Ar), 113.8 – 114.9 (Ar*C meta* to CH_2OAr, 3,4-(3′,4′,5′)-positions, Ar*C ortho* to CH_2 and O on crown ether, Ar*C meta* to CH_2 on crown ether), 115.8 (Ar*C* (2) *ortho* to CO_2CH_2Ar), 121.6 (Ar*C ipso* to CO_2CH_2Ar, Ar*C ortho* to CH_2 on crown ether), 124.2 (Ar*C* (6) *ortho* to CO_2CH_2Ar), 128.9 (Ar*C ipso* to CH_2CO_2Ar on crown ether), 129.1 – 130.1 (Ar*C ipso* to CH_2OAr, 3,4-(3′,4′,5′)-positions, Ar*C ortho* to CH_2OAr, 3,4-(3′,4′,5′)-positions), 131.9 (Ar*C para* to CH_2OAr, 3,4-positions), 138.1 (Ar*C ipso* to CH_2OAr, 3,4-positions), 149.0 (Ar*C meta* (3) to CO_2CH_2Ar), 149.2 (Ar*C ipso* O on crown ether), 153.1 (Ar*C meta* to CH_2OAr, 3,4-positions, Ar*C para* to CO_2CH_2Ar), 158.8 (Ar*C para* to CH_2OAr, 3,4-(3′,4′,5′)-positions), 166.0 (CO_2CH_2Ar); elemental analysis calcd (%) for $C_{150}H_{218}O_{21}$: C 76.43, H 9.32; found: C 76.45, H 9.28.

4′-Methylbenzo[15]crown-5 3,5-bis{3′,4′,5′-tris[*p*-(*n*-dodecan-1-yloxy)benzyloxy]benzyloxy}benzoate [(4-3,4,5-3,5)12G2-B15C5]: **(4-3,4,5-3,5)12G2-CO_2H** (1.5 g, 0.72 mmol), 4′-hydroxymethylbenzo[15]crown-5 (0.26 g, 0.87 mmol), DPTS (68 mg, 0.22 mmol), and DCC (0.22 g, 1.1 mmol) were heated at reflux in CH_2Cl_2 (40 mL) for 10 h. A white crystal (1.40 g, 82.4 %) was obtained after flash column chromatography (silica gel, CH_2Cl_2) and recrystallization in a mixture of CH_2Cl_2 and acetone (1:1, 25 mL). Thermal transitions and corresponding enthalpy changes are reported in Table 2. Purity (HPLC), 99 + %. TLC (1:1 hexane/EtOAc): $R_f = 0.38$; ^{1}H NMR ($CDCl_3$, TMS): $\delta = 0.89$ (t, 18 H, $J = 6.9$ Hz, CH_3), 1.28 (m, 108 H, $CH_3(CH_2)_9$), 1.79 (m, 12 H, CH_2CH_2OAr), 3.76 (s, 8 H, $(OCH_2CH_2)_2$), 3.90 – 3.99 (m, 16 H, CH_2CH_2OAr, $ArOCH_2CH_2O$), 4.18 (m, 4 H, $ArOCH_2CH_2O$), 4.94 (s, 4 H, $ArCH_2OAr$, 3,5-positions), 4.96 (s, 4 H, $ArCH_2OAr$, 3,5-(4′)-positions), 5.03 (s, 8 H, $ArCH_2OAr$, 3,5-(3′,5′)-positions), 5.28 (s, 2 H, CO_2CH_2Ar), 6.74 – 6.79 (m, 9 H, Ar*H meta* to CH_2OAr, 3,5-(4′)-positions, Ar*H ortho* to CH_2OAr, 3,5-positions, Ar*H para* to CO_2CH_2Ar), 6.84 (m, 9 H, Ar*H meta* to CH_2OAr, 3,5-(3′,5′)-positions, Ar*H meta* to CH_2), 7.01 (d, 2 H, $J = 8.1$ Hz, Ar*H ortho* to CH_2), 7.26 – 7.35 (m, 14 H, Ar*H ortho* to CH_2OAr, 3,5-(3′,4′,5′)-positions, Ar*H ortho* to CO_2CH_2Ar); ^{13}C NMR ($CDCl_3$, TMS): $\delta = 14.0$ (CH_3), 22.6 (CH_2CH_3), 26.1 ($CH_2CH_2CH_2OAr$), 29.3 ($CH_3(CH_2)_2CH_2$), 29.6 ($CH_3(CH_2)_3(CH_2)_5$), 30.4 (CH_2CH_2OAr), 31.9 ($CH_3CH_2CH_2$), 66.8 (CO_2CH_2Ar), 68.1 (CH_2CH_2OAr, 3,5-[3′,4′,5′-(4″)]-positions), 69.3, 69.6, 70.6 (crown ether), 71.2 ($ArCH_2OAr$, 3,5-positions), 71.4 ($ArCH_2OAr$, 3,5-(3′,5′)-positions), 74.8 ($ArCH_2OAr$, 3,5-(4′)-positions), 107.4 (Ar*C para* to CO_2CH_2Ar), 107.8 (Ar*C ortho* to CH_2OAr, 3,5-positions), 108.8 (Ar*C ortho* to CO_2CH_2Ar), 113.9 (Ar*C ortho* to CH_2 and O on crown ether), 114.2 – 114.9 (Ar*C meta* to CH_2OAr, 3,5-(3′,4′,5′)-positions, Ar*C meta* to CH_2 on crown ether), 121.7 (Ar*C ortho* to CH_2 on crown ether), 129.1 – 130.5 (Ar*C ipso* to CH_2OAr, 3,5-(3′,4′,5′)-positions, Ar*C ortho* to CH_2OAr, 3,5-(3′,4′,5′)-positions, Ar*C para* to CH_2OAr, 3,5-positions, Ar*C ipso* to CH_2CO_2Ar on crown ether), 131.8 (Ar*C ipso* to CO_2CH_2Ar), 153.2 (Ar*C meta* to CH_2OAr, 3,5-positions), 159.0 (Ar*C para* to CH_2OAr, 3,5-(3′,4′,5′)-positions), 159.8 (Ar*C meta* to CO_2CH_2Ar), 166.1 (CO_2CH_2Ar); elemental analysis calcd (%) for $C_{150}H_{218}O_{21}$: C 76.43, H 9.32; found: C 76.39, H 9.36.

4′-Methylbenzo[15]crown-5 3,4,5-tris{3′,4′,5′-tris[*p*-(*n*-dodecan-1-yloxy)-benzyloxy]benzyloxy}benzoate [(4-3,4,5-3,4,5)12G2-B15C5]: Starting from **(4-3,4,5-3,4,5)12G2-CO_2H** (1.5 g, 0.49 mmol) and 4′-hydroxymethylbenzo[15]crown-5 (0.18 g, 0.59 mmol) in the presence of DPTS (46 mg, 0.15 mmol) and DCC (0.20 g, 0.98 mmol) in CH_2Cl_2 (40 mL) at room temperature for 16 h, a white crystal (0.86 g, 52.5 %) was obtained after flash column chromatography (silica gel, CH_2Cl_2) and recrystallization from a mixture of CH_2Cl_2 and acetone (1:2, 25 mL). Thermal transitions and corresponding enthalpy changes are reported in Table 2. Purity (HPLC), 99 + %; TLC (hexane/ethyl acetate 1:1): $R_f = 0$; ^{1}H NMR ($CDCl_3$, TMS): $\delta = 0.90$ (t, 27 H, $J = 6.8$ Hz, CH_3), 1.28 (m, 162 H, $CH_3(CH_2)_9$), 1.77 (m, 18 H, CH_2CH_2OAr), 3.76 (s, 8 H, $(OCH_2CH_2)_2$), 3.82 – 3.92 (m, 22 H, CH_2CH_2OAr, $ArOCH_2CH_2O$), 4.13 (m, 4 H, $ArOCH_2CH_2O$), 4.75 (s, 6 H, $ArCH_2OAr$, 4-(3′,4′,5′)-positions), 4.86 (s, 4 H, $ArCH_2OAr$, 3,5-(4′)-positions), 4.92 (s, 8 H, $ArCH_2OAr$, 3,5-(3′,5′)-positions), 5.06 (s, 6 H, $ArCH_2OAr$, 3,4,5-positions), 5.27 (s, 2 H, CO_2CH_2Ar), 6.68 – 6.84 (m, 23 H, Ar*H meta* to CH_2OAr, 3,4,5-(3′,4′,5′)-positions, Ar*H ortho* to CH_2OAr, 3,5-positions, Ar*H meta* to CH_2), 6.95 (br s, 2 H, Ar*H ortho* to CH_2), 7.16 – 7.28 (m, 20 H, Ar*H ortho* to CH_2OAr, 3,4,5-(3′,4′,5′)-positions, Ar*H ortho* to CH_2OAr, 4-position), 7.43 (s, 2 H, Ar*H ortho* to CO_2CH_2Ar); ^{13}C NMR ($CDCl_3$, TMS): $\delta = 14.1$ (CH_3), 22.7 (CH_2CH_3), 26.1 – 30.3 ($(CH_2)_8$), 31.9 ($CH_3CH_2CH_2$), 66.8 (CO_2CH_2Ar), 68.0 (CH_2CH_2OAr, 3,4,5-(3′,4′,5′)-positions), 69.0, 69.2, 69.6, 70.5, 70.8 (crown ether), 71.1 ($ArCH_2OAr$, 3,4,5-(3′,5′)-positions), 71.6 ($ArCH_2OAr$, 3,5-positions), 74.8 ($ArCH_2OAr$, 3,4,5-(4′)-positions), 75.1 ($ArCH_2OAr$, 4-position), 107.0 (Ar*C ortho* to CH_2OAr, 3,5-positions), 107.5 (Ar*C ortho* to CH_2OAr, 4-position), 110.0 (Ar*C ortho* to CO_2CH_2Ar), 114.0 (Ar*C ortho* to CH_2 and O on crown ether), 114.2 – 114.4 (Ar*C meta* to CH_2OAr, 3,4,5-(3′,4′,5′)-positions, Ar*C meta* to CH_2 on crown ether), 121.7 (Ar*C ortho* to CH_2 on crown ether), 125.7 (Ar*C ipso* to CO_2CH_2Ar), 128.8 (Ar*C ipso* to CH_2CO_2Ar on crown ether), 129.2 – 130.1 (Ar*C ortho* to CH_2OAr and Ar*C ipso* to CH_2OAr, 3,4,5-(3′,4′,5′)-positions), 132.1 (Ar*C para* to CH_2OAr, 3,4,5-positions), 138.5 (Ar*C ipso* to CH_2OAr, 3,4,5-positions), 142.5 (Ar*C para* to CO_2CH_2Ar), 149.1 (Ar*C ipso* O on crown ether), 152.5 (Ar*C meta* to CO_2CH_2Ar), 152.9 (Ar*C meta* to CH_2OAr, 4-position), 153.2 (Ar*C meta* to CH_2OAr, 3,5-positions), 158.9 (Ar*C para* to CH_2OAr, 3,4,5-(3′,4′,5′)-positions), 166.2 (CO_2CH_2Ar); elemental analysis calcd (%) for $C_{214}H_{314}O_{28}$: C 77.08, H 9.49; found: C 77.11, H 9.48.

Preparation of complexes of monodendrons containing crown ether with NaOTf: Complexes of crown ether monodendrons with NaOTf were prepared by mixing a solution of the dendritic crown ether (ca. 24 mg mL^{-1}) in anhydrous THF with an appropriate volume of a 0.01 M stock solution of

0947-6539/02/0809-2024 $ 20.00+.50/0 *Chem. Eur. J.* **2002**, *8*, No. 9

NaOTf in THF. The solvent was evaporated under a gentle N_2 stream, and the resulting complexes were further dried in a vacuum desicator under vacuum for 24 h at room temperature.

Acknowledgement

Financial support by the National Science Foundation (DMR-99-96288 and DMR-0102459), MURI-ARO, ONR, the Engineering and Physical Science Research Council (UK), and the Synchrotron Radiation Source at Daresbury (UK) are gratefully acknowledged. We are also grateful to Professor S. Z. D. Cheng of the University of Akron for density measurements.

[1] a) G. R. Newkome, C. N. Moorefield, F. Vögtle, *Dendritic Molecules. Concepts*, *Synthesis*, *Perspectives*, VCH, Weinheim, **1996**; b) D. K. Smith, F. Diederich, *Chem. Eur. J.* **1998**, *4*, 1353; c) M. Fischer, F. Vögtle, *Angew. Chem.* **1999**, *111*, 934; *Angew. Chem. Int. Ed.* **1999**, *38*, 884; d) S. Hecht, J. M. J. Fréchet, *Angew. Chem.* **2001**, *113*, 76; *Angew. Chem. Int. Ed.* **2001**, *40*, 74; e) D. Astruc, F. Chardac, *Chem. Rev.* **2001**, *101*, 2991; f) G. E. Oosterom, J. N. H. Reek, P. C. J. Kamer, P. W. N. M. van Leeuwen, *Angew. Chem.* **2001**, *113*, 1878; *Angew. Chem. Int. Ed.* **2001**, *40*, 1828; g) F. Vögtle, *Dendrimers* in *Top. Curr. Chem.* **1998**, *197*; h) F. Vögtle, *Dendrimers II*, *Architecture*, *Nanostructure and Supramolecular Chemistry* in *Top. Curr. Chem.* **2000**, *210*; i) F. Vögtle, in *Dendrimers III*, *Design*, *Dimension*, *Function* in *Top. Curr. Chem.* **2001**, *212*; j) D. Seebach, P. B. Rheiner, G. Greiveldinger, T. Butz, H. Sellner, *Top. Curr. Chem.* **1998**, *197*, 125; k) J. S. Moore, *Acc. Chem. Res.* **1997**, *30*, 402.

[2] a) V. Percec, G. Johansson, J. Heck, G. Ungar, S. V. Batty, *J. Chem. Soc. Perkin Trans. 1* **1993**, 1411; b) G. Johansson, V. Percec, G. Ungar, D. Abramic, *J. Chem. Soc. Perkin Trans. 1* **1994**, 447; c) G. Ungar, S. V. Batty, V. Percec, J. Heck, G. Johansson, *Adv. Mater. Opt. Electron.* **1994**, *4*, 303; d) D. Tomazos, G. Out, J. Heck, G. Johansson, V. Percec, M. Möller, *Liq. Cryst*. **1994**, *16*, 509; e) V. Percec, G. Johansson, G. Ungar, J. Zhou, *J. Am. Chem. Soc.* **1996**, *118*, 9855; f) V. S. K. Balagurusamy, G. Ungar, V. Percec, G. Johansson, *J. Am. Chem. Soc.* **1997**, *119*, 1539; g) S. D. Hudson, H.-T. Jung, V. Percec, W.-D. Cho, G. Johansson, G. Ungar, V. S. K. Balagurusamy, *Science* **1997**, *278*, 449; h) V. Percec, W.-D. Cho, P. E. Mosier, G. Ungar, D. J. P. Yeardley, *J. Am. Chem. Soc.* **1998**, *120*, 11061; i) V. Percec, C.-H. Ahn, T. K. Bera, G. Ungar, D. J. P. Yeardley, *Chem. Eur. J.* **1999**, *5*, 1070; j) G. Ungar, V. Percec, M. N. Holerca, G. Johansson, J. Heck, *Chem. Eur. J.* **2000**, *6*, 1258; k) V. Percec, W.-D. Cho, M. Möller, S. A. Prokhorova, G. Ungar, D. J. P. Yeardley, *J. Am. Chem. Soc.* **2000**, *122*, 4249; l) V. Percec, W.-D. Cho, G. Ungar, D. J. P. Yeardley, *Angew. Chem.* **2000**, *112*, 1661; *Angew. Chem. Int. Ed.* **2000**, *39*, 1597; m) V. Percec, W.-D. Cho, G. Ungar, *J. Am. Chem. Soc.* **2000**, *122*, 10273; n) V. Percec, W.-D. Cho, G. Ungar, D. J. P. Yeardley, *J. Am. Chem. Soc.* **2001**, *123*, 1302; o) W.-J. Pao, M. R. Stetzer, P. A. Heiney, W.-D. Cho, V. Percec, *J. Phys Chem. B* **2001**, *105*, 2170.

[3] a) V. Percec, C.-H. Ahn, G. Ungar, D. J. P. Yeardley, M. Möller, S. S. Sheiko, *Nature* **1998**, *391*, 161; b) V. Percec, C.-H. Ahn, W.-D. Cho, A. M. Jamieson, J. Kim, T. Leman, M. Schmidt, M. Gerle, M. Möller, S. A. Prokhorova, S. S. Sheiko, S. Z. D. Cheng, A. Zhang, G. Ungar, D. J. P. Yeardley, *J. Am. Chem. Soc*. **1998**, *120*, 8619; c) V. Percec, D. Schlueter, G. Ungar, S. Z. D. Cheng, A. Zhang, *Macromolecules* **1998**, *31*, 1745; d) V. Percec, M. N. Holerca, *Biomacromolecules* **2000**, *1*, 6; e) V. Percec, J. A. Heck, D. Tomazos, G. Ungar, *J. Chem. Soc. Perkin Trans. 2* **1993**, 2381; f) V. Percec, D. Tomazos, J. Heck, H. Blackwell, G. Ungar, *J. Chem. Soc. Perkin Trans. 2* **1994**, 31; g) V. Percec, D. Schlueter, Y. K. Kwon, J. Blackwell, M. Möller, P. J. Slangen, *Macromolecules* **1995**, *28*, 8807; h) G. Johansson, V. Percec, G. Ungar, J. P. Zhou, *Macromolecules* **1996**, *29*, 646; i) S. A. Prokhorova, S. S. Sheiko, A. Mourran, R. Azumi, U. Beginn, G. Zipp, C.-H. Ahn, M. N. Holerca, V. Percec, M. Möller, *Langmuir* **2000**, *16*, 6862; j) D. J. P. Yeardley, G. Ungar, V. Percec, M. N. Holerca, G. Johansson, *J. Am. Chem. Soc.* **2000**, *122*, 1684; k) H. Duan, S. D. Hudson, G. Ungar, M. N. Holerca, V. Percec, *Chem. Eur. J.* **2001**, *7*, 4134; l) V. Percec, M. N. Holerca, S. Uchida, S. N. Magonov, D. J. P. Yeardley, G. Ungar, H. Duan, S. D. Hudson, *Biomacromolecules* **2001**, *2*, 706; m) V. Percec, M. N. Holerca, S. Uchida, D. J. P. Yeardley, G. Ungar, *Biomacromolecules* **2001**, *2*, 729.

[4] a) V. Percec, G. Zipp, G. Johansson, U. Beginn, M. Möller, *Macromol. Chem. Phys.* **1997**, *198*, 265; b) U. Beginn, G. Zipp, M. Möller, G. Johansson, V. Percec, *Macromol. Chem. Phys.* **1997**, *198*, 2839; c) V. Percec, T. K. Bera, *Biomacromolecules* **2002**, *3*, 167.

[5] a) V. Percec, P. Chu, G. Ungar, J. Zhou, *J. Am. Chem. Soc*. **1995**, *117*, 11441; b) V. Percec, M. Kawasumi, *Macromolecules* **1992**, *25*, 3843; c) V. Percec, C. G. Cho, C. Pugh, D. Tomazos, *Macromolecules* **1992**, *25*, 1164; d) V. Percec, P. Chu, M. Kawasumi, *Macromolecules* **1994**, *27*, 4441.

[6] a) H. H. Tinh, C. Destrade, *Mol. Cryst. Liq. Lett.* **1989**, *6*, 123; b) G. Staufer, M. Schellhorn, G. Lattermann, *Liq. Cryst.* **1995**, *18*, 519.

[7] H. H. Tinh, C. Destrade, J. Malthête, *Liq. Cryst.* **1990**, *6*, 797.

[8] a) J. Malthête, N. H. Tinh, A. M. Levelut, *J. Chem. Soc. Chem. Commun.* **1986**, 1548; b) J. Malthête, A. Collet, A. M. Levelut, *Liq. Cryst.* **1989**, *5*, 123.

[9] G. Ungar, D. Abramic, V. Percec, J. A. Heck, *Liq. Cryst.* **1996**, *21*, 73.

[10] V. Percec, A. Keller, *Macromolecules* **1990**, *23*, 4347.

[11] J.-M. Lehn, *Supramolecular Chemistry*, VCH, New York, **1995**.

[12] a) C. F. van Nostrum, R. J. M. Nolte, *Chem. Commun.* **1996**, 2385; b) D. Lelièvre, L. Bosio, J. Simon, J.-J. André, F. Bensebaa, *J. Am. Chem. Soc.* **1992**, *114*, 4475; c) J. Simon, M. K. Engel, C. Soulié, *New J. Chem.* **1992**, *16*, 287; d) J. Simon, C. Sirlin, *Pure Appl. Chem.* **1989**, *61*, 1625; e) V. Balzani, A. Credi, F. M. Raymo, J. F Stoddart, *Angew. Chem.* **2000**, *112*, 3486; *Angew. Chem. Int. Ed.* **2000**, *39*, 3348; f) J.-P Sauvage, *Acc. Chem. Res.* **1998**, *31*, 611; g) A. Liebmann, C. Mertesdorf, T. Plesnivy, H. Ringsdorf, J. H. Wendorff, *Angew. Chem.* **1991**, *103*, 1358; *Angew. Chem. Int. Ed. Engl.* **1991**, *30*, 1375.

[13] I. Gitsov, P. T. Ivanova, *Chem. Commun.* **2000**, 269.

[14] For selected examples of dendrimers that self-organize in liquid crystalline phases see for example: a) D. J Pesak, J. S. Moore, *Angew. Chem.* **1997**, *109*, 1709; *Angew. Chem. Int. Ed.* **1997**, *36*, 1636; b) H. Meier, M. Lehmann, *Angew. Chem.* **1998**, *110*, 666; *Angew. Chem. Int. Ed.* **1998**, *37*, 643; c) J. Barberá, M. Marcos, J. L. Serrano, *Chem. Eur. J.* **1999**, *5*, 1834; d) M. Marcos, R. Giménez, J. L. Serrano, B. Donnio, B. Heinrich, D. Guillon, *Chem. Eur. J.* **2001**, *7*, 1006; e) M. Suárez, J.-M. Lehn, S. C. Zimmerman, A. Skoulios, B. Heinrich, *J. Am. Chem. Soc.* **1998**, *120*, 9526; f) R. Deschenaux, E. Serrano, A.-H. Levelut, *Chem. Commun.* **1997**, 1577; g) M. W. P. L. Baars, S. H. M. Söntjens, H. M. Fischer, H. W. I. Peerlings, E. W. Meijer, *Chem. Eur. J.* **1998**, *4*, 2456; h) I. M. Saez, J. W. Goodby, R. M. Richardson, *Chem. Eur. J.* **2001**, *7*, 2758.

Received: October 10, 2001 [F3603]